This preprint has been submitted for review to the International Journal of Earth Sciences.

Mesozoic paleogeography, structural configuration and evolution of the central Northern Calcareous Alps (Eastern Alps, Austria): Alternative scenarios and discussion

Oscar Fernandez[1], Hugo Ortner[2], Diethard Sanders[2], Bernhard Grasemann[1], Thomas Leitner[3]

[1]Dept. of Geology, University of Vienna, Josef-Holaubek-Platz 2 (UZA II), 1090 Vienna, Austria.

[2]Dept. of Geology, University of Innsbruck, Innrain 52f, 6020 Innsbruck, Austria.

[3]Salinen AG, Altaussee 139, 8992 Altaussee, AUSTRIA

ORCIDs: OF, 0000-0003-1584-2684; HO, 0000-0001-6909-6627; DS, 0000-0002-4620-1110; BG, 0000-0002-4647-8224.

Corresponding author e-mail: oscar.fernandez.bellon@univie.ac.at

Twitter: @itsoscarsfault

Mesozoic paleogeography, structural configuration and evolution of the central Northern Calcareous Alps (Eastern Alps, Austria): Alternative scenarios and discussion

Oscar Fernandez[1], Hugo Ortner[2], Diethard Sanders[2], Bernhard Grasemann[1], Thomas Leitner[3]

[1]Dept. of Geology, University of Vienna, Josef-Holaubek-Platz 2 (UZA II), 1090 Vienna, Austria.

[2]Dept. of Geology, University of Innsbruck, Innrain 52f, 6020 Innsbruck, Austria.

[3]Salinen AG, Altaussee 139, 8992 Altaussee, AUSTRIA

ORCIDs: OF, 0000-0003-1584-2684; HO, 0000-0001-6909-6627; DS, 0000-0002-4620-1110; BG, 0000-0002-4647-8224.

Corresponding author e-mail: oscar.fernandez.bellon@univie.ac.at

Abstract

One of the most remarkable features of the central Northern Calcareous Alps (Eastern Alps, Austria) is the widespread presence of Upper Triassic deep-water carbonates and Permo-Triassic evaporites resting on deep-water Middle Jurassic sediments and their underlying Upper Triassic shallow-water carbonate platform successions. The Triassic deep-water carbonates and accompanying evaporites have been classically interpreted to originate either from a location south of the time-equivalent carbonate platforms, or to have been deposited in deeper water seaways within the broader platform domain. To date, this dispute has been addressed mostly through the analysis of Triassic and Jurassic facies distribution in map view, which, however, is subject to some degree of ambiguity and subjectivity. In this contribution we present, for the first time, balanced and sequentially restored cross-sections through the central Northern Calcareous Alps to understand the implications of the contrasting paleogeographic models. We present: (a) an interpretation based on a highly allochthonous origin of the Triassic deep-water units; and (b) an interpretation based on their relative autochthony. The restored cross-sections highlight those aspects in each interpretation that need further research. The allochthonous-origin interpretation requires a structural evolution that fails to account for all available constraints. The relative autochthonous-origin interpretation must rest on a concept of deep-water carbonate deposition in intraplatform seaways that satisfactorily accounts for the observed Triassic facies distribution.

KEYWORDS: Eastern Alps, cross-sections, thrust tectonics, salt tectonics, gravitational gliding, structural uncertainty

STATEMENTS AND DECLARATIONS

Competing interests: The authors declare no conflict of interest.

Data availability: Geological maps used for cross-section construction are openly available from www.geologie.ac.at. Field dip data and revised mapping is available from the corresponding author upon request.

Authorship: Conceptualization: All Authors; Methodology: Oscar Fernandez, Hugo Ortner; Formal analysis and investigation: All Authors; Writing - original draft preparation: Oscar Fernandez, Hugo Ortner; Writing - review and editing: All Authors; Funding acquisition: Oscar Fernandez, Thomas Leitner, Bernhard Grasemann; Resources: All Authors; Supervision: Oscar Fernandez.

ACKNOWLEDGMENTS

Research is supported by the FFG and Salinen AG through the FFG-Bridge Project ETAPAS (FO999888049), by FWF Project POLARIS (I 5399-N), and by project Structure and Deformation of Salt-bearing Rifted Margins (SABREM), PID2020-117598GB-I00, funded by MCIN/ AEI /10.13039/501100011033. The authors wish to thank K. Decker, M. Habermüller and W. Schöllnberger for enriching discussion, and Petex for academic license access for IPM-Move that was used for the construction and restoration of cross-section. Christian Schneider is thanked for kindly granting use to his photo of the Hachelwand, and Sonangol for use of the seismic profile of the offshore Kwanza basin.

Introduction

Tectono-sedimentary relationships are key indicators to unravel the tectonic evolution of fold-and-thrust belts. The Northern Calcareous Alps (NCA) of the Eastern Alps of Austria are no exception, and such relationships for Mesozoic sediments have been widely used to understand their kinematics (e.g., Peresson and Decker 1997; Faupl and Wagreich 2000; Frisch and Gawlick 2003; Schweigl and Neubauer 1997; Frank and Schlager 2006; Froitzheim et al. 2008; Ortner et al. 2008; Gawlick and Missoni 2019). Consensus exists that sediments deposited in the NCA since the Late Jurassic reflect the initiation and progression of the Alpine Orogeny (e.g., Faupl and Wagreich 2000; Frisch and Gawlick 2003). In spite of this general agreement, there still exist diverging views on the pre-Jurassic paleogeography of the NCA, and on the precise nature of Late Jurassic to Early Cretaceous tectonism. These alternative hypotheses have been summarized and discussed, amongst others, by Faupl and Wagreich (2000) and Frisch and Gawlick (2003).

Most of the conflicting paleogeographic reconstructions of the NCA, and the attempts at understanding the NCA's Jurassic to Cretaceous structural evolution, have been driven by map-based analysis of facies distributions of sediments both pre-dating and synchronous to Late Jurassic to Early Cretaceous tectonism (e.g., Zankl 1967; Schlager 1967; Tollmann 1981; Haas et al. 1995; Schweigl and Neubauer 1997; Gawlick et al 1999; Mandl 2000; Frisch and Gawlick 2003). The main controversy hinges on disagreements on the significance of the present-day distribution and on the inferred original distribution of Upper Triassic facies belts. In particular, the disagreement centers on the origin of a suite of Triassic deposits that are grouped informally under the term "Hallstatt facies" (and which will be referred to hereafter as the Hallstatt units). The interpretation on the origin of the Hallstatt units derives in various collateral implications. The Hallstatt units are assemblages of predominantly Upper Triassic deep-water sediments, up to a few hundreds of meters in thickness. The deep-water Hallstatt units can be encountered today in diverse structural relationships with their time-equivalent platform carbonates, but most commonly they are thrust onto the latter. Hallstatt unit occurrences are typically associated with outcrops of Permo-Triassic evaporites and clastics, and of Middle to Upper Jurassic syn-tectonic deposits coeval with emplacement of the Hallstatt units.

The contrast in the depositional environments of Upper Triassic carbonates has been known for over a century and already led Hahn (1913a, b) to identify different tectonic units based on facies differences. Following from the seminal work of Hahn, different interpretations have been put forward since then for the origin of the deep-water Hallstatt units. Based on the interpreted paleogeographic position of the Hallstatt, hypotheses that seek to explain the observed structural relationships between the Hallstatt units and adjacent units can be placed in two groups: a) Hallstatt units accumulated in seaways in between shallow-water carbonate platforms, which implies relative autochthony of the Hallstatt units (e.g., Schlager 1967; Schweigl and Neubauer 1997); or b) a single Hallstatt facies belt deposited in a halokinetically active, distal shelf setting immediately south of the platform domain, and emplaced onto the platform succession by northward transport, implying a significant allochthony of the Hallstatt units (e.g., Tollmann 1981; Mandl 2000; Gawlick and Missoni 2019).

To date, however, the precise nature of the structural relationships between the Hallstatt units and their adjacent Triassic and Jurassic units has not been studied systematically. In this contribution we present cross-sections through three of the main accumulations of Hallstatt units in the central NCA, with the aim of evaluating the structural validity of the aforementioned hypotheses. The sections we present include two alternative interpretations, corresponding to concepts of relative autochthony or of allochthony of the Hallstatt units. Based on these sections we describe the inferred tectonic evolution and discuss the implications on the paleogeography of the Hallstatt units and on the structure of the NCA in general.

Geological setting and background

The Eastern Alps comprise a stack of units from three tectonic provinces (Schmid et al. 2008) (Fig. 1c): Europe and its southern passive margin; the Alpine Tethys; and the Austroalpine domain (a segment of the Adria microcontinent). From Triassic to Middle Jurassic time, the Austroalpine domain was characterized by a passive margin that faced southeastwards into the Neotethys (or Meliata Tethys) ocean and, from Early to Late Jurassic times, by a passive margin that faced northwestawrd into the Alpine Tethys (or Penninic) ocean.

The development of the future Eastern Alps started in the Permian, with rifting of the Variscan Orogen and its foreland leading to the opening of the Meliata Tethys, along the southern to eastern edge of the Austroalpine, during the early Middle Triassic (Schmid et al. 2008; Schuster et al. 2019). The Alpine Tethys then opened, during the Early to Late Jurassic, between the Austroalpine and Europe. Partly coeval with opening of the Alpine Tethys,

subduction of the Meliata Tethys initiated in the Late Jurassic (Schmid et al. 2008; Schuster et al. 2019), which led to the first contractional phase in the Austroalpine domain. Subsequently, intra-continental collision and subduction occurred within the Austroalpine domain during the Early Cretaceous (Stüwe and Schuster 2010).

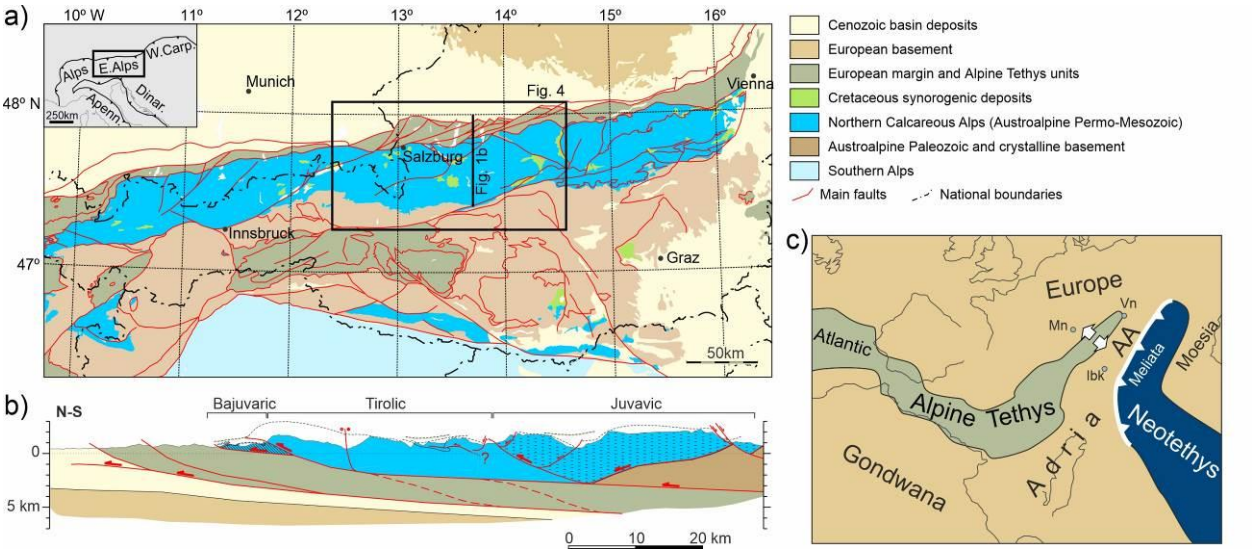

Fig. 1 a Simplified geological map of the Eastern Alps (adapted from Schuster et al. 2015). **b** Synthetic geological cross-section across the central Northern Calcareous Alps. **c** Paleogeographic reconstruction of the Austroalpine (AA) Domain in relation to Europe and surrounding oceans at Late Jurassic times (adapted from Schuster et al. 2019). Ibk: Innsbruck, Mn: Munich, Vn: Vienna

Whereas Early Cretaceous intra-continental subduction is well-documented based on records of metamorphism (Miller and Thöni 1997; Stüwe and Schuster 2010), the precise nature of Late Jurassic tectonism is still debated. In the absence of evidence for metamorphism of this age, authors have based their interpretations on isolated observations of tectono-sedimentary relationships. Interpretations range from either transtension and/or transpression (Frank and Schlager 2006; Ortner et al. 2008; Mandl 2013; Ortner 2017), to subduction with associated thrusting (Gawlick et al. 1999; Frisch and Gawlick 2003), or to accretionary prism development (Gawlick and Missoni 2019).

During the main phase of Alpine orogenesis, lasting from Late Cretaceous to Early Miocene times, the Austroalpine domain was thrust over the Alpine Tethys. Subsequently, both tectonic units together overrode the European margin, whereby the proximal foreland succession became involved in thrusting (Faupl and Wagreich 2000; Schmid et al. 2008; Schuster et al. 2019). A final phase of deformation involved the exhumation of the axial zone of the Eastern Alps and the lateral extrusion along the orogen (Ratschbacher et al. 1991; Schuster et al. 2019).

Within the Eastern Alps, the Northern Calcareous Alps (NCA) are an Upper Permian to Cretaceous sedimentary succession, part of the Austroalpine unit, that has been almost entirely decoupled from its pre-Permian basement. The NCA Permo-Mesozoic lies at present directly above imbricated Alpine Tethys and European units, and, along its trailing edge, above its pre-Permian basement (Fig. 1a,b). The NCA are traditionally sub-divided into three major thrust systems; from lower to higher and from foreland to hinterland these are the Bajuvaric, the Tirolic, and the Juvavic thrust systems (Hahn 1913a,b; Mandl 2000) (Fig. 1b). The reason for this subdivision relates historically to the distribution of Triassic facies, but the need for a revision has been highlighted by several authors (cf., Tollmann 1964; Mandl 2000; Frisch and Gawlick 2003; Ortner and Kilian 2022).

Stratigraphy

The Permo-Mesozoic succession of the NCA (see, e.g., Tollmann 1976a; Mandl 2000; Gawlick et al. 2009) (Fig. 2) was originally underlain by Paleozoic deposits and Variscan units, that presently form most of the antiformal stack of the axial zone of the Eastern Alps. In the NCA, basal successions of Permian red beds are overlain by and Upper Permian to Lower Triassic sequence of evaporites and shallow-marine clastics that ranges in thickness from a few hundreds to more than 1000 m. Above them an Anisian (Middle Triassic) succession up to few 100s of meters in thickness of shallow- and deep-water limestones is present; this succession is interpreted to represent the end of

rifting (Leitner and Spötl 2017; Strauss et al. 2021). The Anisian carbonates, in turn, are overlain by thick (in the order of 1000 m) Ladinian (Middle Triassic) shallow-water carbonate platforms comprising lagoons, reefs, and steep slopes. The Ladinian platforms locally interfinger and prograded over a much thinner package of basinal shales to limestones. During the subsequent Carnian (Late Triassic) pluvial episodes (cf., Ogg 2015), the Ladinian platform-and-basin ensembles became buried with a cyclothemic, mixed siliciclastic-carbonatic-evaporitic succession of highly variable thickness (zero to a few 100s of m) (e.g., Bechstädt and Schweizer 1991).

Next, above the lower to middle Carnian succession, a huge carbonate platform established, that persisted from the late Carnian to the late Norian (Late Triassic). This platform, termed Hauptdolomit-Dachsteinkalk megabank, represents the most widespread carbonate rock unit of the NCA (e.g., Fig. 3), and may attain ~2000 m in thickness. In the central NCA, the platform is represented by the –mostly undolomitized– Dachstein limestone, that comprises peritidal cyclic successions ('lagoonal Dachstein limestone'), reefal to peri-reefal deposits ('reefal Dachstein limestone'), and their slope to proximal basin equivalents. During the Rhaetian stage (Late Triassic), a single large the Hauptdolomit–Dachsteinkalk megabank (cf., Mandl, 2000) became differentiated into shallow basins with intercalated small carbonate shelves. Locally, in contrast, deposition of the Dachstein limestone and its Rhaetian slope to basinal equivalent range up to the top of the Triassic.

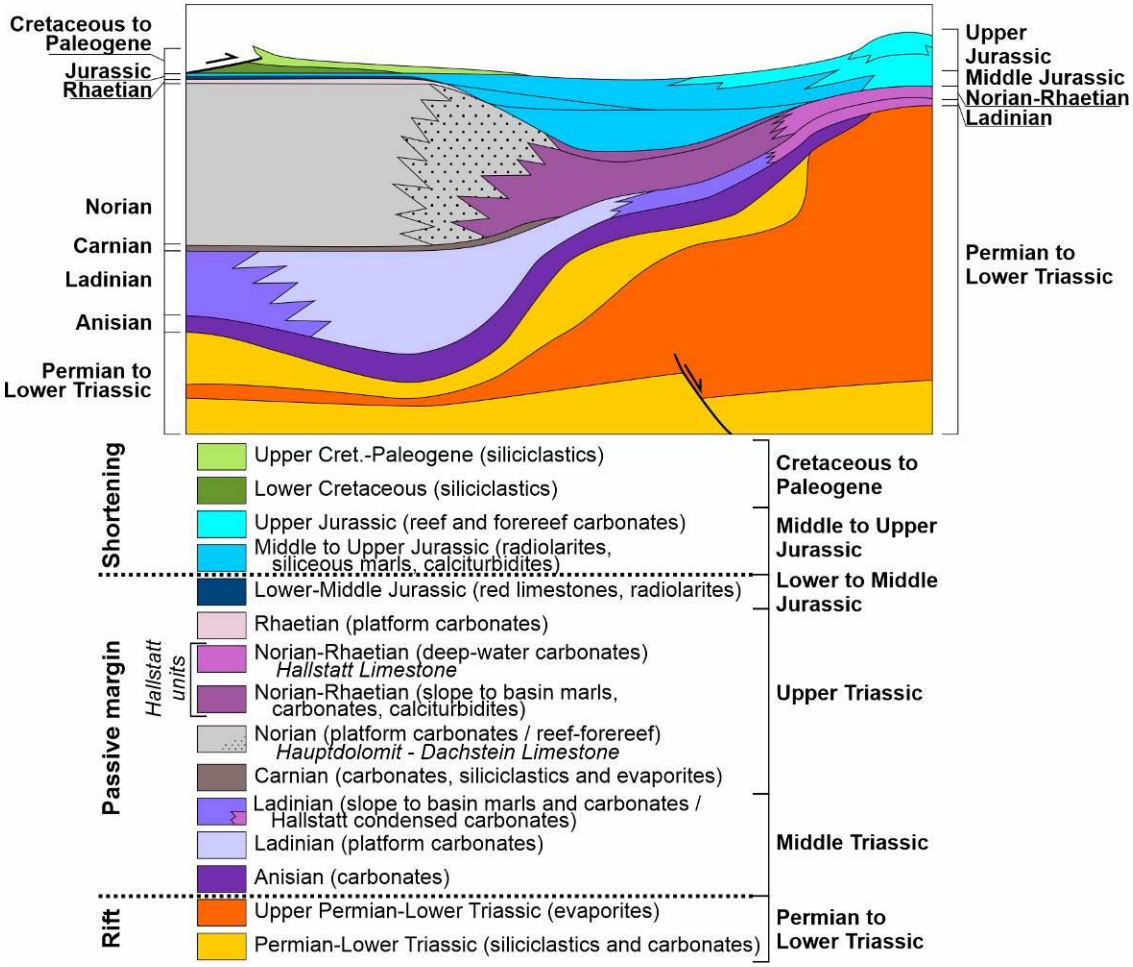

Fig. 2 Synthetic chronostratigraphic chart of the Northern Calcareous Alps (adapted from Mandl 2000 and Fernandez et al. 2022)

In the so-called Hallstatt basins, that corresponded to the Norian and, locally, also to the Ladinian carbonate platforms, diverse types of (locally dolomitized) deep-water limestones traditionally lumped under the term Hallstatt facies (Hallstatt units) accumulated. The archetypical Hallstatt facies (referred to here as the Hallstatt limestone) is a stratigraphically condensed package of wavy-bedded to stylonodular, red-coloured limestones that are rich in fossils, in particular in ammonites. The Hallstatt limestones interfinger with allodapic carbonates shed from the platforms

and their slopes. The original location of the Hallstatt basins relative to the time-equivalent Norian carbonate platforms is debated and the currently existing alternative models will be discussed below.

At the end of Triassic time, the Hauptdolomit-Dachsteinkalk megabank was tectonically segmented and drowned. From the Early to Middle Jurassic, a differentiated seafloor topography gave rise to deposition of packages of condensed, red deep-water limestones (rosso ammonitico) on submarine swells whilst thick successions of cherty deep-water limestones accumulated in the intercalated basins. During the terminal Middle Jurassic, probably mainly due to increased nutrient availability (Baumgartner, 2013), sedimentation switched from calcareous to siliceous (radiolarites, siliceous marls); concomitantly, turbiditic deposition related to contractional tectonism started (Frisch and Gawlick 2003). Continued shortening throughout the Late Jurassic led to local shallowing over structural swells, followed by establishment of isolated carbonate platform-to-slope systems.

The Triassic-Jurassic are covered, mostly unconformably and in separate basins, by synorogenic deposits of Cretaceous to Paleogene age. These units deposited synchronous to Cretaceous to Paleogene thrusting: from initial imbrication of the NCA thrusts (Early Cretaceous) and to decoupling of the NCA from their basement and northward thrusting over the Alpine Tethys (Late Cretaceous to Paleogene) (Faupl and Wagreich 2000). The stratigraphic record associated to Paleogene northward thrusting and Miocene lateral extrusion is absent (eroded) over most of the central NCA (Frisch et al. 1998; Ortner and Stingl 2001; Egger et al. 2017).

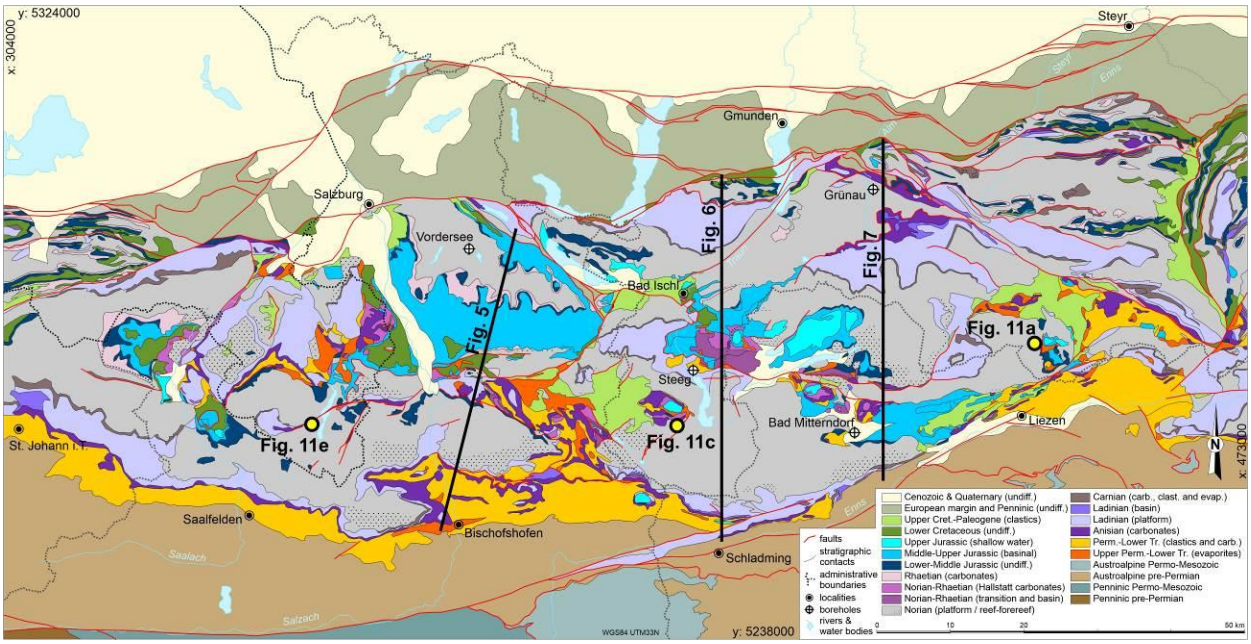

Fig. 3 Geological map of the central Northern Calcareous Alps (adapted from Krenmayr 2005 and Krenmayr and Schnabel 2006)

The controversy on the origin of the Hallstatt units

The Late Triassic paleogeography of the central NCA has been debated for more than a century. The debate hinges on the common presence of Norian Hallstatt units in domains otherwise dominated by Norian shallow-water platform carbonates (lagoonal and reefal Dachstein limestone) (Fig. 4a). The Hallstatt units typically cluster along specific elongate regions that trend roughly NW-SE and NE-SW (Fig. 4a). These regions (referred to traditionally as "Hallstatt zones") are further characterized by abundant Permo-Triassic evaporites (Fig. 4a) and Lower Triassic clastics. Three of these regions are the subject of this contribution: the Lammertal Zone, the Altaussee Zone, and the Bad Mitterndorf Zone ('Lm', 'At', 'BM' in Fig. 4a).

It is consistently observed that the Hallstatt units rest on Middle to Upper Jurassic sediments that in turn blanket the Norian platform units (Mandl et al. 2012; Mandl 2013; Gawlick and Missoni 2015, 2019, Fernandez et al. 2021). Locally, along with Hallstatt units, kilometer-sized blocks of Triassic platform carbonates also rest structurally on Jurassic beds and their underlying Triassic platforms (i.e., a duplication of Triassic platforms; Braun 1998; Gawlick and Missoni 2019; Ortner et al. 2022). Likewise, Permo-Triassic evaporite masses and Lower Triassic clastics,

without associated Hallstatt units, can rest on Jurassic rocks (Mandl et al. 2012; Fernandez et al. 2021; Kurz et al. under review). These juxtapositions are generally interpreted to be the result of transport during Jurassic tectonic activity, although there is no consensus on the exact nature of the transport and the degree of allochthony of the overlying units.

Apart from cropping out near Permo-Triassic evaporites, the Hallstatt units are locally affected by syn-depositional fractures and faults (fractures filled with Norian-age lime mud; Schlager 1969). These observations are generally accepted to indicate that the Hallstatt units formed in a deep-water domain with abundant Permo-Triassic salt with active salt tectonism (e.g., Mandl 2000, Schorn and Neubauer 2014; Gawlick and Missoni 2019). Kenter and Schlager (2009) used observations of the transition from the Dachstein platform into Hallstatt units along the Gosaukamm ('Gk' in Fig. 4a) to deduce that Norian basinal facies formed in water depths of 300-500 m. Based on this, relatively shallow, water depth Kenter and Schlager (2009) concluded that the base of the Hallstatt basin must have been elevated relative to that of the neighboring Dachstein platform. A possible "pedestal" for the Hallstatt basins could be provided by domains of inflated salt (cf., Mandl 2000; Fig. 2). The Gosaukamm transition studied by Kenter and Schlager (2009) is also an important reference point for the Norian depositional model. This is the only fully preserved Upper Triassic platform-to-basin transition in the central NCA, displaying a transition from lagoonal via reefal to slope and basinal environment. The slope and basinal facies (marls, deep water carbonates and turbidites) separate the highly condensed "true" Hallstatt limestones from the platform and reef (as depicted in Fig. 2).

The original geographic location of the evaporite bodies and of the associated Hallstatt units is, however, much less agreed upon. Two competing scenarios exist: a) the Hallstatt units were originally deposited within "channels" (seaways) within the Norian (Dachstein) platforms (a fragmented platform) and were thrusted, locally, onto their neighboring platforms in the Jurassic (concept of relative autochthony) (Zankl 1967; Schlager 1967; Häusler, 1980); and b) the Hallstatt units originally formed a single facies belt along the south-facing margin of the Norian (Dachstein) platform (south of the current outcrop limit of the NCA) before being dismembered and emplaced northwards onto a single Dachstein platform, during the Jurassic (concept of relative allochthony). Within this second scenario, there are in turn alternative views on how the emplacement of the allochthonous Hallstatt units and the Permo-Triassic evaporites occurred. One interpretation assumes that uplift of the distal margin led to the northward gravitational sliding of large fragments (olistoliths) of the allochthonous units into their present-day positions. This is known as the *Gleittektonik* model (Tollmann, 1981; who was inspired by the work of Plöchinger and Draxler 1974). A second interpretation posits that the apparently "chaotic" arrangement of Hallstatt units, evaporites, and a few large blocks derived from the Triassic platforms resulted from amalgamation within a Jurassic accretionary prism emplaced over the NCA, of which only fragments are preserved today (Gawlick et al. 1999; Gawlick and Missoni 2019). Both of these allochthonous interpretations imply that the Hallstatt units (and other allochthonous units) were transported over tens of kilometers into their current positions above the Triassic platforms.

The contrasting autochthonous/allochthonous scenarios imply different views on the Upper Triassic paleogeography. Zankl (1967) illustrated that the relative autochthony scenario implies the presence of several Hallstatt basinal seaways within the shallow-water platform (Fig. 4c). These seaways would correspond to the present-day regions of Hallstatt unit outcrops and are characterized by platform-margin deposits along their northern edges.

In contrast, the scenarios of relative allochthony imply that all Hallstatt units were deposited south of the current southern outcrop margin of the NCA (Fig. 4d). Platform edge facies (reefal Dachstein limestone) in these scenarios correspond to bathymetric variations within the platform (Fig. 4d). The main paleogeographic difference between the *Gleittektonik* (Tollmann 1981) and the accretionary prism (Gawlick and Missoni 2019) sub-scenarios relates to the interpretation of platform units that are at present associated with Hallstatt unit outcrops (Fig. 4d). Tollmann (1981) interpreted the Berchtesgaden-Untersberg-Unken and the Dachstein-Grimming platforms to be greatly allochthonous (Fig. 4d). Frisch and Gawlick (2003) and Missoni and Gawlick (2019) delimit the allochthony of platform units to two smaller platform blocks located at present north of the Tennengebirge platform (the Schwarzer Berg and Hoher Göll, see Fig. 5) also considered allochthonous by Tollmann (1981).

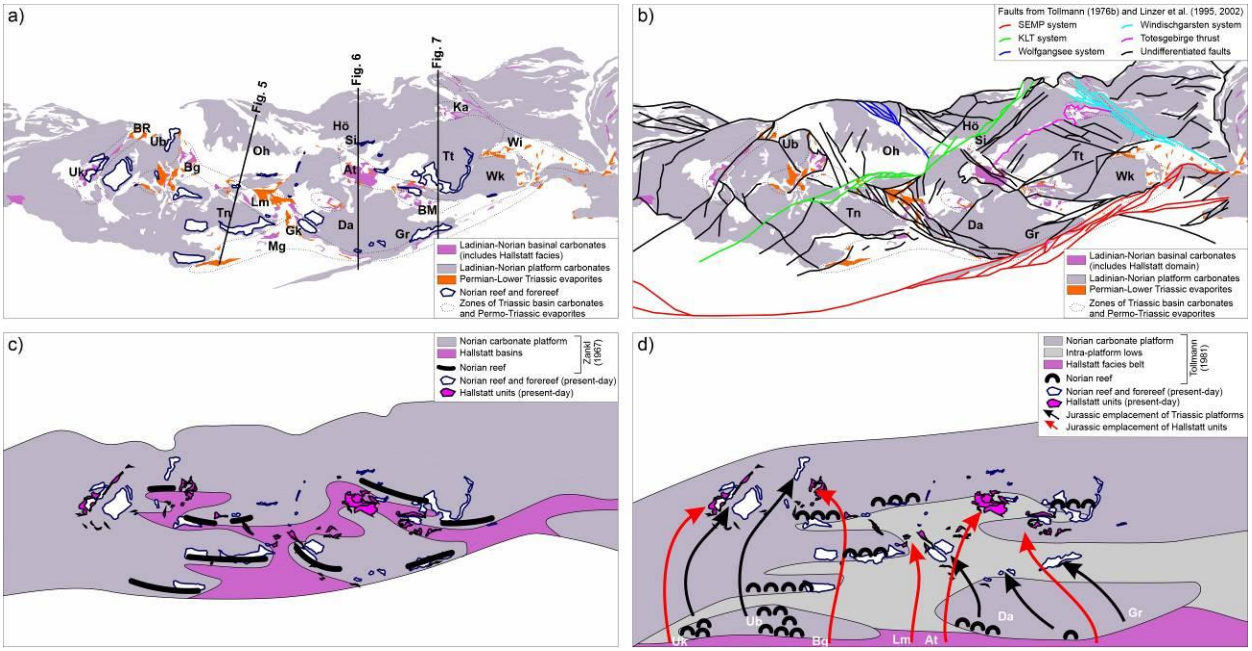

Fig. 4 a Geological map of the central Northern Calcareous Alps (as in Fig. 3) showing the present-day distribution of Middle (Ladinian) to Upper (Norian) Triassic shallow-water platform carbonates, their time-equivalent Hallstatt units, and Permo-Triassic evaporites. Upper Triassic (Norian) reefs have been mapped from published 1:50000 scale geological maps (Plöchinger 1982, 1987; Schäffer 1982; Mandl and Matura 1995; Pavlik 2007, 2009, 2013a, 2013b, 2014; Moser 2014), and correspond to either reef or near-reef facies within the otherwise lagoonal Upper Triassic (Norian) platform. Basinal units crop out in elongated clusters marked by the dashed lines and named informally as: At: Altaussee; Bg: Berchtesgaden; BM: Bad Mitterndorf; BR: Bad Reichenhall; Gk: Gosaukamm; Ka: Kasberg; Lm: Lammertal; Mg: NCA southern margin; Uk: Unken; Wi: Windischgarsten. Blocks of platform domain bounding the basinal domains are labelled as: Da: Dachstein; Gr: Grimming; Hö: Höllengebirge; Oh: Osterhorngruppe; Tn: Tennengebirge; Tt: Totes Gebirge; Si: Singereben; Ub: Untersberg; Wk: Warscheneck. **b** Overlay of the map in **(a)** with the main structures active during the lateral extrusion of the Eastern Alps (taken from Linzer et al. 1995, 2002 and partly from Tollmann 1976b). Note the dominant NE-SW and NW-SE trends, and the coincidence of some of the key fault corridors with the zones of basinal carbonate outcrops. **c** Highlighted distribution of Upper Triassic (Norian) reefs and representation of the Hallstatt basins according to Zankl (1967). The map-sketch of Zankl (1967) has been adapted to fit the actual geography of the NCA such that the location of his Hallstatt basins and Norian reefs is comparable to those on the geological map from **(a)**. **d** Highlighted distribution of Upper Triassic (Norian) reefs and representation of the "true" Hallstatt (Eo-Hallstatt) and Mio-Hallstatt channels according to Tollmann (1981). The map-sketch of Tollmann (1981) has been adapted to fit the actual geography of the NCA such that the location of his Norian reefs is comparable to those on the geological map from **(a)**. Arrows indicate approximate transport of allochthonous units and connect equivalent features in their Triassic and present-day location

Regional cross-sections

Background considerations

Despite decades of debate on the origin of the Hallstatt units in the central NCA, and efforts to illustrate the competing alternative models (e.g., Zankl 1967, Tollmann 1981, Frisch and Gawlick 2003), there has been no attempt to date to systematically investigate the structural architecture of the area. In an attempt to shed new light on this debate, we present cross-sections along three transects in the central NCA.

The cross-sections are traced in a roughly N-S direction. This implies that there is potentially out-of-plane motion across the section planes, as shortening has varied from NW-directed to NE-directed (Linzer et al. 1995; Peresson and Decker 1997). Furthermore, the most recent stage of Miocene lateral extrusion of the Eastern Alps led to offset along NE-SW and NW-SE directed fault corridors (Ratschbacher et al. 1991; Linzer et al. 1995, 2002; Peresson and Decker 1997; Frisch and Gawlick 2003) (Fig. 4b). Notwithstanding, the net effect in the central NCA is one of roughly N-S shortening, as can be inferred from the roughly E-W trend of the NCA at regional scale, the

approximate E-W trend of the structures along the leading edge of the central NCA (Fig. 3), and the south-directed dip of the base of the Alpine foreland basin (Brix and Schulz 1993). Furthermore, Miocene strike-slip offsets within the NCA are less than ten kilometers on individual fault systems (Linzer et al. 2002; Levi et al. 2022). This is a length scale smaller than the tens of kilometers of width of the Triassic platform and basin units shown in Fig. 4a. Therefore, when restored, Miocene strike-slip offset does not significantly alter the present-day relative arrangement of the different Triassic platform and basin units (e.g., Frisch and Gawlick 2003).

Linzer et al. (1995), who have published the only balanced structural cross-section through the central NCA, opted for a NW-SE directed cross-section direction based on the inference that most of the early shortening in the NCA was NW-directed. However, the location and orientation picked by these authors for their cross-section avoided the "problem" of the Hallstatt units. In contrast, the North-South orientation chosen in this contribution allows us to display the critical contacts between Hallstatt units and their underlying Triassic carbonate platforms. This implies that, if the directions of transport documented by previous authors are correct, balance cannot be expected for the cross-sections presented here.

The three cross-section traces presented here (Fig. 3) intend to illustrate: the Lammertal Zone and its relationship to its adjacent Osterhorngruppe and Tennegebirge platform blocks (Fig. 4a); the Altausee Zone and its relationship to its adjacent Singereben and Dachstein platform blocks (Fig. 4a); and the Bad Mitterndorf Zone and its relationship to its adjacent Totes Gebirge and Grimming platform blocks (Fig. 4a).

The three cross-sections are interpreted for two alternative scenarios: one scenario is compatible with the *Gleittektonik* allochthony model of Tollmann (1981) and the accretionary prism model of Gawlick and Missoni (2019); the second scenario seeks to represent a concept of relative autochthony of the Hallstatt units.

In the allochthony scenario, Triassic units (both shallow-water and deep-water carbonates) resting on Jurassic rocks are interpreted to have been transported from south of the NCA southern margin (Figs. 5b, 6b, 7b). Furthermore, the allochthonous Triassic units are interpreted to be of variable thickness due to deposition in a patchy arrangement, above thick Permo-Triassic evaporites south of the Upper Triassic platform, tens of kilometers south of their present location (Mandl 2000) (Fig. 4d). In contrast, the platform units underlying Jurassic rocks are interpreted to be of roughly constant thickness and to be continuous across the entire study area (even where overlain by other units). No significant Permo-Triassic evaporites are expected to exist or to have existed beneath the Triassic platforms. The difference in the interpreted emplacement mechanisms of the *Gleittektonik* (gravitational sliding) and the accretionary prism (thrust emplacement) sub-scenarios have no consequence on the relationship between the allochthonous units and the underlying platforms.

The autochthony scenario assumes that Hallstatt units are thinner than their time-equivalent Triassic platform units and were deposited above Permo-Triassic salt bodies. The salt bodies that floor the Hallstatt units were subsiding structures located between domains of shallow-water platform deposition. These salt bodies are at present significantly laterally shortened. It is also interpreted that the Triassic platforms developed atop Permo-Triassic salt that has been mostly evacuated through halokinesis. This scenario requires less total shortening than the allochthony model but in contrast interprets some structures to record S-directed thrusting (i.e., backthrusts) (Figs. 5c, 6c, 7c).

Both scenarios concur that the NCA are detached from their pre-Permian basement (other than along their trailing edge) and that they are at present thrust over thrust sheets derived from the Penninic ocean and the European continental passive margin. This has been shown by numerous wells drilled in the NCA, including the Vordersee and Grünau wells within the study area (Hamilton 1989; Egger et al. 2009) (Figs. 3, 5, 7). The basal thrust of the NCA is interpreted to be of low angle, based on the fact that the Mesozoic stratigraphy is relatively constant in thickness and lies at a steady elevation from foreland to hinterland (Figs. 5-7; Fernandez et al. 2022) and a tabular seismic velocity structure documented by deep refraction profile Alp01 for the central NCA (Brückl et al. 2007). The basal NCA thrust was interpreted to dip with ~1° by Linzer et al. (1995) and similar values are used in our interpretation.

Linzer et al. (1995, 2002) interpreted that the Miocene strike-slip fault-systems detached along the Alpine thrusts, an inference that is independent of the structural scenario. The key Miocene fault systems cross-cut by the cross-sections are the KLT (Königssee-Lammertal-Traunsee) and the Windischgarsten fault systems (Decker 1994; Linzer et al 1995, 2002; Levi et al. 2022) (Figs. 4b, 5-7). The SEMP (Salzach-Enns-Mariazell-Puchberg) fault system (Fig. 4b), which is interpreted to accommodate many tens of kilometers of offset (Linzer et al. 2002), defines the southern limit of Sections 2 and 3. The Wolfgangsee system (Fig. 4b), in turn, is the northern limit of Section 1. Along both

the Wolfgangsee and Windischgarsten fault systems, sub-NCA Penninic and distal European margin units are locally exposed (Plöchinger 1964; Linzer et al. 1995, 2002; Peresson and Decker 1997). These fault systems are therefore interpreted to be rooted in the lowermost Alpine thrusts (Figs. 5, 7).

Section 1: Osterhorngruppe-Lammertal-Tennengebirge

The westernmost section crosses the Lammertal Zone (Fig. 4a), a NW-SE trending belt of outcrops of Permo-Triassic evaporites and clastics, Anisian carbonates, Hallstatt units, and a large block (Schwarzer Berg) of Triassic platform (Fig. 5). The northern margin of the Lammertal Zone is riddled with E-W trending post-Cretaceous faults that mask its relationship with the Osterhorngruppe platform block to the North (Fig. 5). To the South instead, the units of the Lammertal Zone rest, across tectonic contacts, on Middle Jurassic siliceous marls (Fig. 5) that, in turn, veneer the Triassic platform of the Tennengebirge (Fig. 5). The structurally lowermost (southernmost) of the tectonic contacts is many kilometers in length and can be traced along the entire length of the northern margin of the Tennegebirge block, and farther west across the Salzach valley (Fig. 3).

These contacts have been interpreted in the framework of the allochthony scenario as, either, surfaces of gravitational sliding (Ortner et al. 2022) or as the base of an accretionary prism (Gawlick and Missoni 2019) (as illustrated in Fig. 5b). In this scenario, all the elements of the Lammertal Zone were emplaced from farther south, and structurally overlie the Triassic of the Tennengebirge and the Osterhorngruppe (Fig. 5b).

In a scenario of autochthony (Fig. 5c), in contrast, the Lammertal Zone is backthrust onto the Tennengebirge and the platform block of the Schwarzer Berg represents the southern prolongation of the Osterhorngruppe Triassic platform.

Another main difference between both models relates to lateral variations in thickness of the Middle to Upper Triassic interval. This interval varies from nearly 5 km in thickness at the Vordersee well, to less than 3.5 km in thickness on the southern edge of the Tennengebirge (Fig. 5b,c). These units are generally accepted to post-date rifting (Leitner and Spötl 2017; Strauss et al. 2021). Therefore, thickness changes have been made gradual in the allochthony scenario (Fig. 5b) but have been allowed to relate to thickness variations in the underlying Permo-Triassic evaporites in the autochthony scenario (Fig. 5c).

A third significant difference relates to the structure of the southern end of the cross-sections (south of the Tennengebirge), for which two tentative alternative interpretations are presented. This is an area in which outcrop conditions are relatively poor, but geological mapping reveals the repeated presence of Anisian carbonates and Permo-Triassic clastics and evaporites. This is conventionally interpreted to be a zone of pervasive thrust imbrication (e.g. Mandl 1998) and represented as such in the allochthony scenario (Fig. 5b). In the autochthony scenario, an alternative structure consisting of tilted salt-floored mini-basins with intervening welded diapirs is proposed (Fig. 5c).

Finally, the northern end of the section varies between both scenarios, to reflect possible alternatives. The cross-section intentionally ends south of the Wolfgangsee fault system (Fig. 4b) that exposes units underlying the basal NCA thrust at the surface (Plöchinger 1964; Linzer et al. 1995, 2002; Peresson and Decker 1997). This fault system was interpreted to consist of steeply dipping faults (Linzer et al. 1995, 2002; Peresson and Decker 1997). We have assumed sub-vertical dip for the Wolfgangsee faults in the allochthony scenario (beyond the northern end of Fig. 5b), and propose an alternative interpretation for the Wolfgangsee fault system as out-of-sequence thrusts, with lower dips, in the allochthony scenario (Fig. 5c).

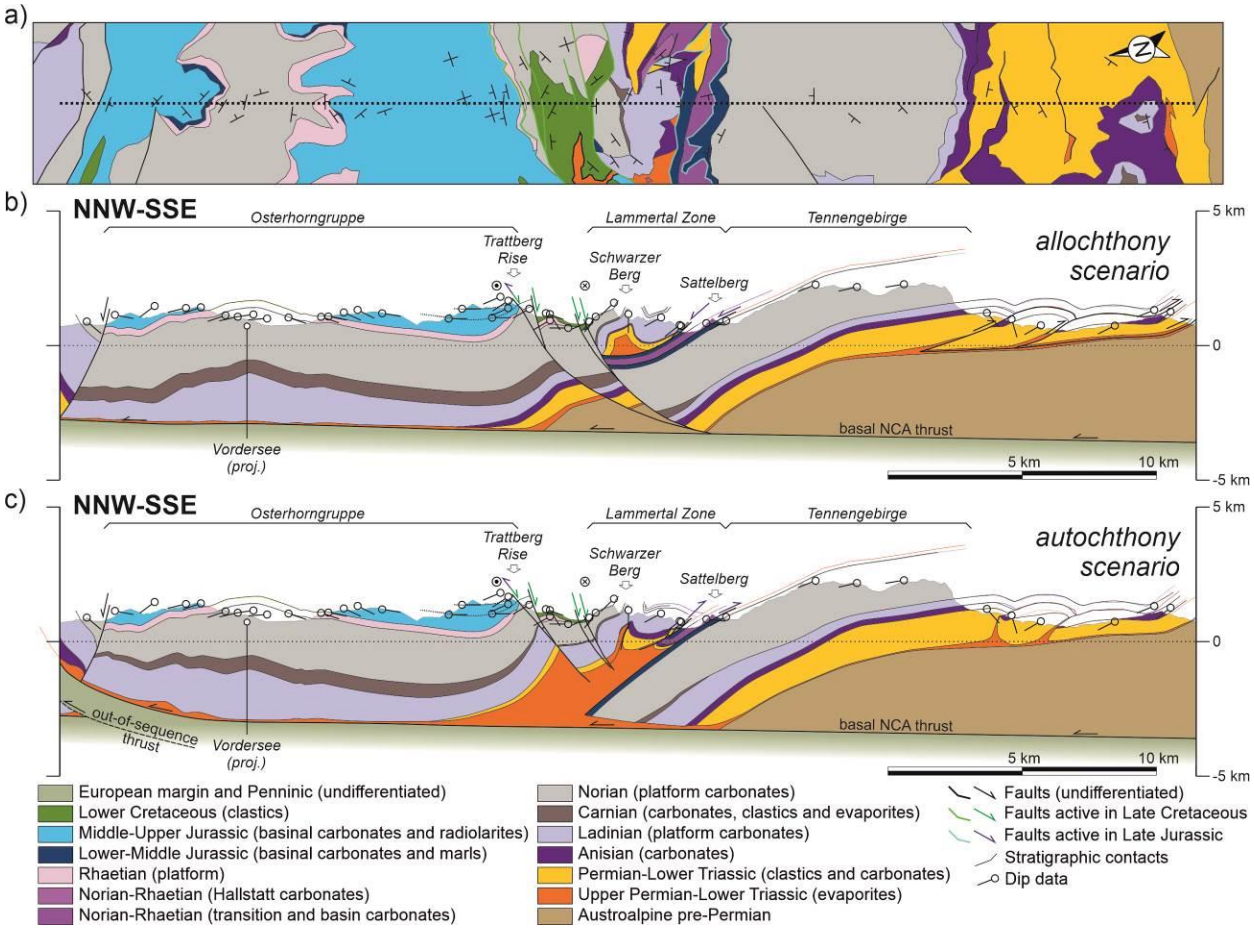

Fig. 5 a Simplified geological map along cross-section 1. Adapted from Plöchinger (1987), Egger and van Husen (2003), and Krenmayr (2013). **b** Interpretation of cross-section 1 according to a scenario of allochthony of the Lammertal Zone units. **c** Interpretation of cross-section 1 according to a scenario of relative autochthony of the Lammertal Zone units

Section 2: Höllengebirge-Altaussee-Dachstein

The central section (Fig. 6) crosses the Altaussee Zone (Fig. 4a), an area in which Triassic Hallstatt units crop out extensively, surrounded and overlain mainly by Middle to Upper Jurassic rocks. This section also cuts across the Dachstein thrust sheet, a unit that was emplaced onto the Altaussee Zone from Early Cretaceous times onwards (Mandl 2000; Fernandez et al. 2022), with continued activity up to Miocene times (Decker et al. 1994; Levi et al. 2022).

In the allochthony scenario (Fig. 6b), the Altaussee Zone rests, entirely decoupled from its original root, on the southern prolongation of the Höllengebirge-Singereben unit, as shown by Mandl et al. (2012). The Höllengebirge-Singereben unit extends south, under the Dachstein thrusts sheet, and rests on the pre-Permian Austroalpine basement that crops out along the southern edge of the NCA.

In the autochthony scenario (Fig. 6c), the Altaussee Zone is floored by Permo-Triassic evaporites and is folded and thrusted a few kilometers northward onto the Höllengebirge-Singereben unit. In this scenario it is interpreted that the Dachstein thrust sheet lies directly on the pre-Permian Austroalpine basement of the southern end of the section.

As with Section 1, two alternative interpretations are presented for the structure of the Lower Triassic and Anisian at the southern end of the section (beneath the Dachstein unit). In the allochthony model (Fig. 6b), the imbricate model of Mandl (1998) has been preferred. Furthermore, the imbricates are interpreted to be part of the Höllengebirge-Singereben unit (Mandl 1998). In the autochthony model (Fig. 6c), an alternative of squeezed and partly thrusted diapirs, with intervening minibasins with thick Permo-Triassic clastics, has been used.

Likewise, thickness changes observed, or inferred in the Triassic platforms have been dealt with as in Section 1. In the allochthony scenario they have been resolved with gradual variations in thickness, conditioning the geometry of the basal thrust of the NCA under the Höllengebirge (Fig. 6b). In the autochthony scenario, in contrast, the Triassic platforms have been allowed to vary in thickness more freely, resulting in a thinner Triassic stratigraphy beneath the Singereben, thinning into the Altaussee and variable thickness in the Dachstein thrust sheet (Fig. 6c).

This section shows two noteworthy features, highlighted with insets in Fig. 6b,c. One is the presence of Hallstatt limestone directly overlying the Triassic platform succession in the leading edge of the Dachstein thrust sheet. The Hallstatt limestone here is found in the hanging wall of an extensional fault immediately north of the Hoher Sarstein. Mandl (2003) interpreted this fragment of Hallstatt limestone to be allochthonous, whereas Fernandez et al. (2022) suggest that it was deposited locally atop the Norian platform carbonates. The Hallstatt limestone is in turn overlain by Middle to Upper Jurassic sediments (Schlagintweit and Gawlick 2006).

The second feature are exposures of Upper Jurassic reefal limestones and Upper Cretaceous clastics along the trailing edge of the Dachstein thrust sheet, in the area of Ramsau (Mandl 1998, Mandl et al 2014). These sediments lie directly on Lower Triassic clastics, and form slivers separated by faults from the Dachstein unit to the North and the Mandlingzug to the South. The Mandlingzug itself is a structural block along the SEMP fault system with a stratigraphy that differs from the neighboring Dachstein unit and has been interpreted to derive from west of the study area (e.g., Frisch and Gawlick 2003)

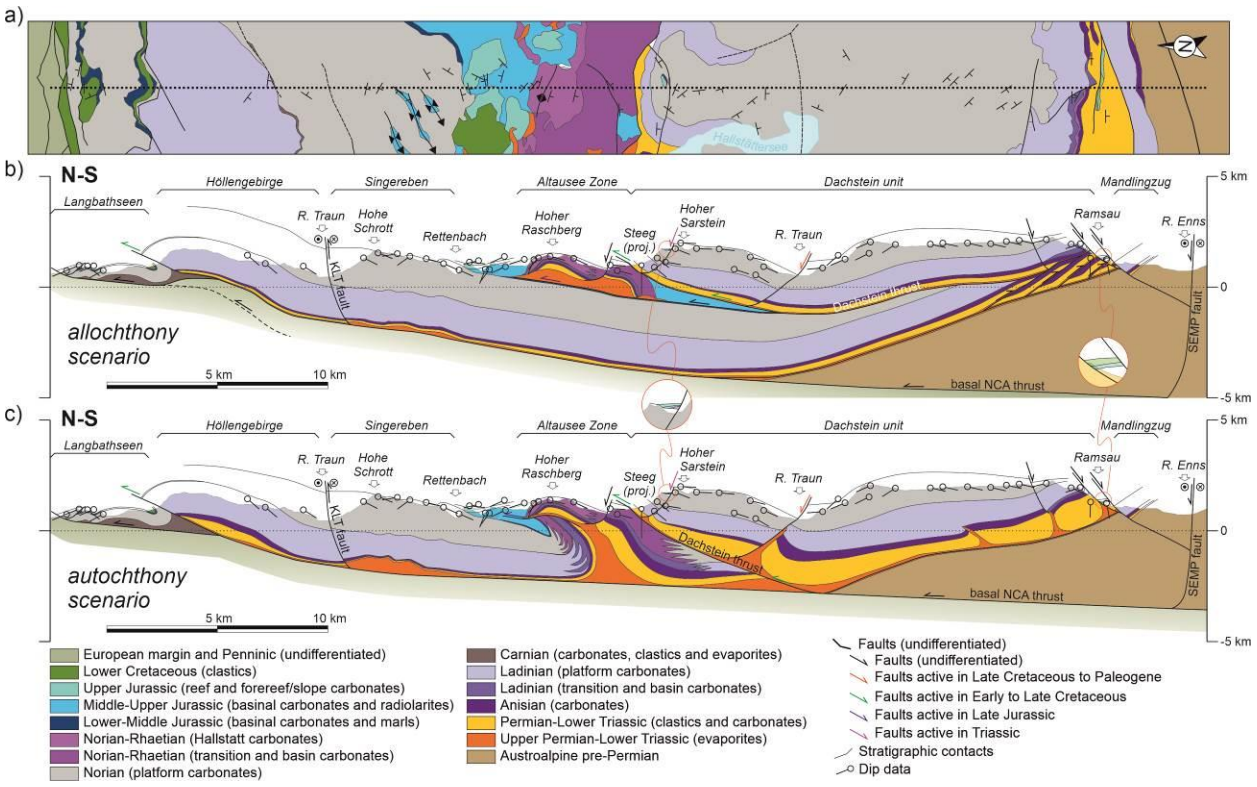

Fig. 6 a Simplified geological map along cross-section 2. Adapted from Schäffer (1982), Mandl and Matura (1995), and Egger (1996). **b** Interpretation of cross-section 2 according to a scenario of allochthony of the Altaussee zone units. **c** Interpretation of cross-section 2 according to a scenario of relative autochthony of the Altaussee zone units

Section 3: Kasberg-Totesgebirge-Bad Mitterndorf

The western section (Fig. 7) crosses the Bad Mitterndorf Zone (Fig. 4a), an area in which Triassic Hallstatt units crop out in a patchy arrangement in association with Upper Jurassic sediments (Fig. 3). The interpretation on this cross-section is supported by two deep boreholes: the Grünau-1 and the Bad Mitterndorf TH-1 wells (Hamilton 1989; Schmid et al. 2003). The Grünau-1 well indicates a thickening of the Carnian and confirms the absence of Ladinian platform carbonates in the subsurface of the Kasberg area (Fig. 7b,c). This well also penetrated the basal NCA thrust, the underlying allochthonous European margin and Penninic units and their basal thrust, and the

autochthonous foreland above the European basement. The Bad Mitterndorf TH-1 well in turn drilled a thick Middle to Upper Triassic succession that forms part of the Grimming unit (Fig. 7b, c) but failed to reach the basal NCA thrust.

As with the previous cross-sections, the nature of emplacement of the Hallstatt units varies depending on the assumed model. In the allochthony scenario, the Bad Mitterndorf and Tauplitzalm units rest allochthonously on Norian carbonates of the Totesgebirge-Grimming unit (Fig. 7b). Although Tollmann (1960) and Schmid (2003) interpreted the Tauplitzalm units to be part of the Totesgebirge-Grimming unit, an allochthonous origin is proposed here based on the absence of the Ladinian, the persistent outcrop of Carnian, and a thin Upper Triassic stratigraphy (Tollmann 1960; Schöllnberger 1973; Moser 2014).

In the autochthony scenario, the Tauplitzalm constitutes the southern prolongation of the Totesgebirge (similar to the relationship between the Schwarzer Berg and the Osterhorngruppe in Section 1). The Tauplitzalm unit is thrust northwards onto the Totesgebirge, and the rocks of the Bad Mitterndorf Zone are backthrust onto the Grimming unit (Fig. 7c).

In both scenarios, the basal surface of the Bad Mitterndorf Zone is sealed by Upper Jurassic sediments. In contrast, the thrust transporting the Tauplitzalm unit northwards post-dates the Upper Jurassic, and may correlate in age with the Dachstein thrust of Section 2, although with smaller displacement.

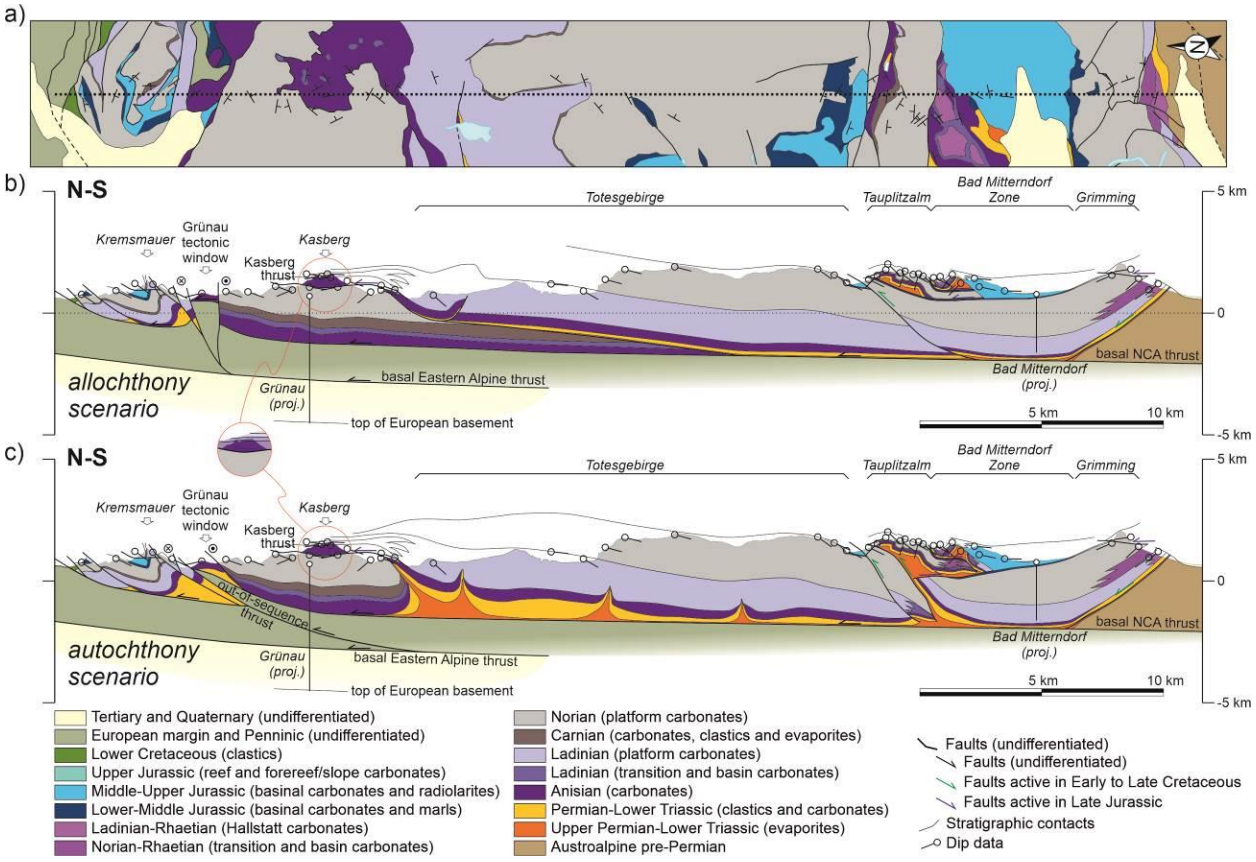

Fig. 7 a Simplified geological map along cross-section 3. Adapted from Egger and Van Husen (2007), Moser (2014), and Kreuss (2020). **b** Interpretation of cross-section 3 according to a scenario of allochthony of the Bad Mitterndorf zone units and absent salt in the Kasberg thrust. **c** Interpretation of cross-section 3 according to a scenario of relative autochthony of the Bad Mitterndorf zone units and a salt-fed thrust model for the Kasberg thrust.

North of the Bad Mitterndorf Zone and the Tauplitzalm, the Triassic reaches nearly 4 km in thickness in the Totesgebirge unit (Fig. 7b, c). Although Linzer et al. (1995) interpreted this stratigraphy to be tectonically duplicated, they did so by interpreting unexplained thickness variations within the Triassic. Evidence for such a tectonic duplication (e.g., in the form of large-displacement low-angle thrusting) is absent within the Totesgebirge

(Schäffer 1982; Egger and van Husen 2007; Moser and Pavlik 2013; Moser 2014). Nonetheless, the entire Totesgebirge unit is part of the hangingwall of the Kasberg thrust (named Totesgebirge thrust by Tollmann 1976b) (Fig. 7b, c). This thrust places Middle Triassic (Anisian and Ladinian) rocks on Upper Triassic (Norian) carbonates with a flat-on-flat geometry and northwest-directed transport direction (Fig. 7b, c) (Linzer et al. 1995). The obliquity of emplacement relative to the section trace is solved in the allochthony scenario with the interpretation of a highly oblique ramp at depth (Fig. 7b). In the autochthony scenario, the Kasberg thrust is interpreted to be a salt-fed thrust (Fig. 7c). Permo-Triassic salt and clastics crop out at multiple locations immediately west of the cross-section (Fig. 7a; Egger and van Husen 2007; Moser 2014) making this a reasonable possibility.

Finally, two possible alternative interpretations are presented for the Grünau tectonic window (Fig.7b, c), wherein sub-NCA units (European margin and Penninic units) are exposed along the Windischgarsten fault system (Linzer et al. 1995). One possible interpretation contemplates a strike-slip system rooted in the basal Alpine thrust (Fig. 7b). The other interpretation assumes the presence of an out-of-sequence thrust cutting up-section from the basal Alpine thrust (Fig. 7c), akin to the structural sketch of Hamilton (1989).

Structural evolution of the central NCA

The three presented cross-sections (Figs. 5-7) show that the available outcrop and borehole data can be fit with two strongly contrasting structural interpretations. As discussed above, cross-section balancing is of limited applicability to reduce uncertainty in this setting due to significant amounts of out-of-plane motion. As an alternative to balancing, we have used sequential restoration of the interpreted cross-sections to understand the implications that each interpretation would have on our understanding of the tectonic evolution of the NCA.

Restoration methodology

The objective of sequential restoration is to understand the geometric and tectonic relationships among the main structural units of the NCA through time. The restorations have intentionally left out elements north of the Wolfgangsee and Windischgarsten systems (in Figs. 8 and 10) and south of the SEMP system (in Figs. 9 and 10) to reduce complexity related to these Miocene strike-slip systems. The restorations performed simplify tectonic shortening to it being north-directed (parallel to the direction of cross-sections) and focus on understanding the evolving relationships between structural units. Only qualitative magnitudes of tectonic shortening can be extracted from these restorations.

The relationships between syn-tectonic sediments and the structures depicted on the cross-sections in Figs. 5-7, along with work from previous authors (Tollmann 1981; Mandl 2000; Linzer et al. 1995, 2002; Krische and Gawlick 2015; Ortner 2017; Gawlick and Missoni 2015, 2019), have been used to reconstruct the structural evolution. The restored geometries shown in Figs. 8-10 have been obtained by inverse modelling, that is by removing deformation progressively, from present to past. The restorations have been performed by unfolding of fault blocks using a flexural flow algorithm (Griffiths et al. 2002), and the fault block restoration method discussed in Lingrey and Vidal-Royo (2015). The restoration has resulted in gaps and overlaps between fault blocks that are well under 5% of section length. These are considered irrelevant and have been removed from the presented results. In contrast, significant gaps or overlaps (in excess of 10% of section length) are highlighted on the sections. These are area-balance problems that are large enough that they potentially indicate a problem with the interpretation and need to be addressed in a full three-dimensional analysis which is beyond the scope of this paper. Segments between fault blocks that have been eroded since Jurassic times are not considered balance errors, and they have been interpolated or extrapolated during reconstruction.

Three restored steps have been generated for each cross-section (Figs. 8-10). One is at Late Cretaceous to Paleogene times, by which time deformation internal to the NCA, other than Neogene strike-slip tectonics, had already taken place (Faupl and Wagreich 2000; Stüwe and Schuster 2010; Schuster et al. 2019) and the NCA had been decoupled from their Austroalpine basement and thrust over the Penninic units (Figs. 8b, f, 9b, f, 10b, f). The second restoration step is one at the end of the Late Jurassic, by which time the Hallstatt units had already been emplaced on the Triassic platforms (Figs. 8c, g, 9c, g, 10c, g). The final restoration step is the end of the Late Triassic, a time at which the original relationship between the Upper Triassic platforms and their time equivalent Hallstatt units in depositional state can be illustrated (Figs. 8d, h, 9d, h, 10d, h). This last step relates to the paleogeographies shown in Fig. 4c, d. For this restored state, the top of the Triassic platforms is interpreted to have been near sea level, whereas the Hallstatt units deposited up to depths of around 500 m.

Lower and Upper Cretaceous sediments crop out at present only in isolated patches scattered along the NCA (Fig. 3). The range of elevation of remaining outcrops (ranging roughly from 1500 to 500 m above sea level; Schäffer 1982) however, hints at a potentially originally thick (1000 m or more) and broad cover of Cretaceous sediments that potentially filled in much of the orogenic topography of the NCA. On the restored cross-sections, a top of Cretaceous sediments is suggested (with a gently foreland-directed dip <1°) based on this assumption (Figs. 8b, f, 9b, f, 10b, f).

The geometry of the base of the NCA in the three different restoration stages is significantly unconstrained. However, the following guidelines have been used in the restoration process. For the Late Cretaceous-Paleogene step a basal NCA thrust geometry similar to the present one has been assumed. Deformation interpreted to relate to sub-NCA structures has been removed. For the Late Jurassic and Late Triassic steps, the base of the NCA rested on the Austroalpine basement. The geometry of the basement is uncertain and has been inferred to be parallel to the base of the NCA Permo-Triassic succession in the allochthony scenario. In the autochthony scenario, a flat top of basement has been interpreted where possible, with a variable thickness of Permo-Triassic salt above it. In both scenarios, the possible presence of pre-Ladinian rift faults offsetting the basement is indicated where thickness changes are rapid (e.g., from the Lanbathseen to Höllengebirge units in Fig. 9d, h). In the autochthony scenario, possible basement faults are also contemplated below inferred salt structures in the autochthony scenario (e.g., below the Lammertal Zone in Fig. 8h), assuming that, they might have controlled the nucleation of salt structures due to differences in the original thickness of Permo-Triassic salt across them. Some basement features are interpreted to have been inverted during Jurassic shortening.

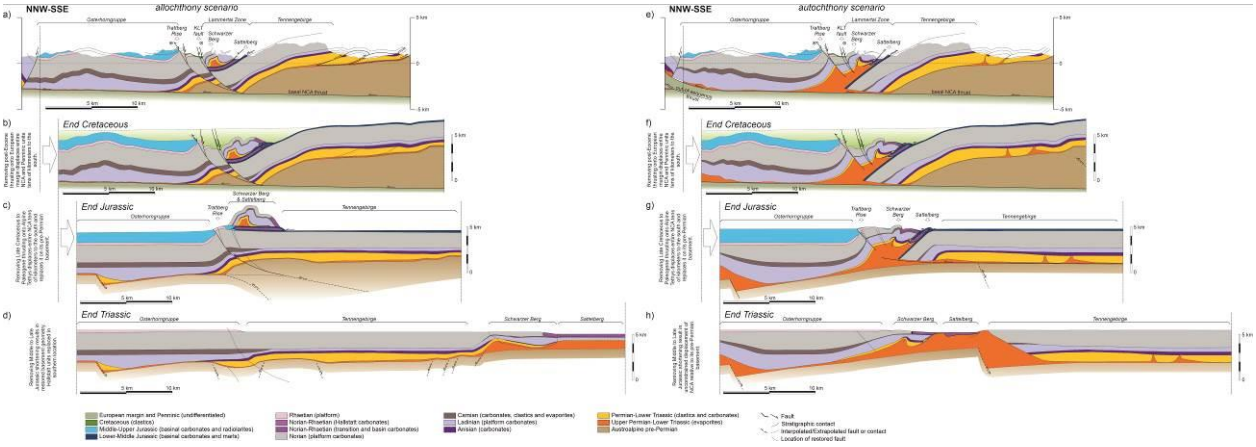

Fig. 8 Restorations of Section 1 for both alternative scenarios. See text for details. **a** Section 1 in its present-day geometry, interpreted based on the allochthony scenario. **b** Restoration of Section 1 (allochthony scenario) to a time equivalent to the end of the Cretaceous or in the Paleogene. **c** Restoration of Section 1 (allochthony scenario) to a time equivalent to the end of the Jurassic. **d** Restoration of Section 1 (allochthony scenario) to a time equivalent to the end of the Triassic. **e** Section 1 in its present-day geometry, interpreted based on the autochthony scenario. **f** Restoration of Section 1 (autochthony scenario) to a time equivalent to the end of the Cretaceous or in the Paleogene. **g** Restoration of Section 1 (autochthony scenario) to a time equivalent to the end of the Jurassic. **h** Restoration of Section 1 (autochthony scenario) to a time equivalent to the end of the Triassic

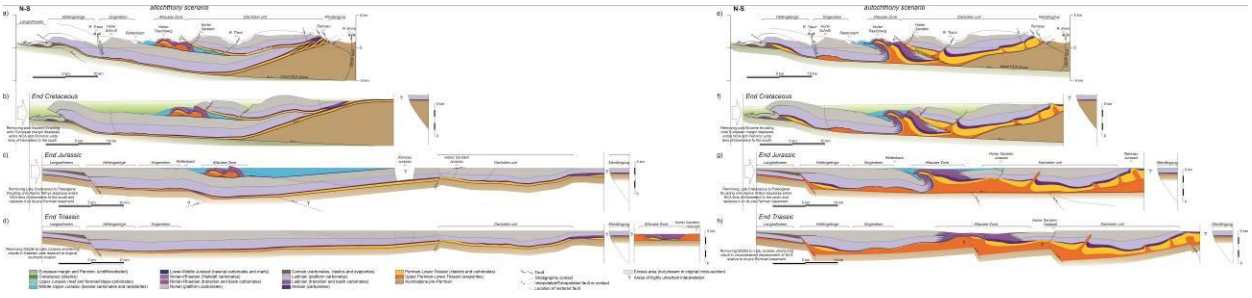

Fig. 9 Restorations of Section 2 for both alternative models. See text for details. **a** Section 2 in its present-day geometry, interpreted based on the allochthony scenario. **b** Restoration of Section 2 (allochthony scenario) to a time

equivalent to the end of the Cretaceous or in the Paleogene. **c** Restoration of Section 2 (allochthony scenario) to a time equivalent to the end of the Jurassic. **d** Restoration of Section 2 (allochthony scenario) to a time equivalent to the end of the Triassic. **e** Section 2 in its present-day geometry, interpreted based on the autochthony scenario. **f** Restoration of Section 2 (autochthony scenario) to a time equivalent to the end of the Cretaceous or in the Paleogene. **g** Restoration of Section 2 (autochthony scenario) to a time equivalent to the end of the Jurassic. **h** Restoration of Section 2 (autochthony scenario) to a time equivalent to the end of the Triassic

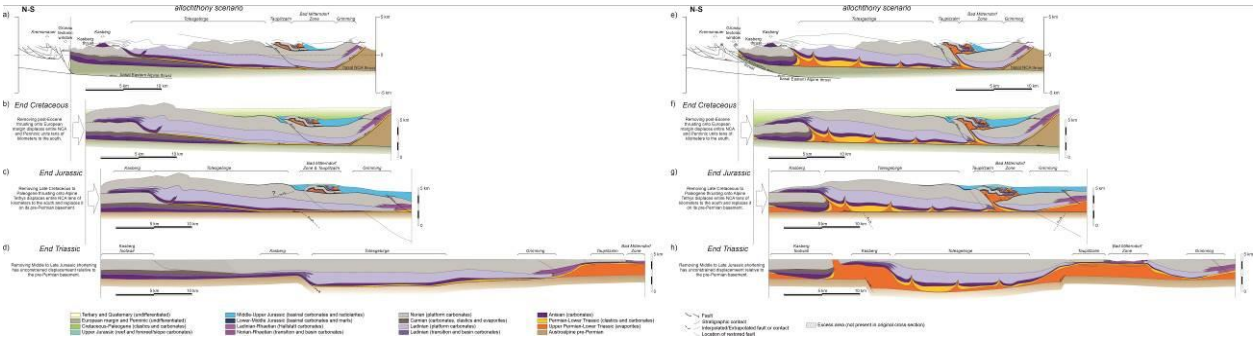

Fig. 10 Restorations of Section 3 for both alternative models. See text for details. **a** Section 3 in its present-day geometry, interpreted based on the allochthony scenario. **b** Restoration of Section 3 (allochthony scenario) to a time equivalent to the end of the Cretaceous or in the Paleogene. **c** Restoration of Section 3 (allochthony scenario) to a time equivalent to the end of the Jurassic. **d** Restoration of Section 3 (allochthony scenario) to a time equivalent to the end of the Triassic. **e** Section 3 in its present-day geometry, interpreted based on the autochthony scenario. **f** Restoration of Section 3 (autochthony scenario) to a time equivalent to the end of the Cretaceous or in the Paleogene. **g** Restoration of Section 3 (autochthony scenario) to a time equivalent to the end of the Jurassic. **h** Restoration of Section 3 (autochthony scenario) to a time equivalent to the end of the Triassic

Results of the restoration

It is not our objective here to discuss the restorations in Figs. 8-10 in detail. We concentrate instead on the higher-order features or critical elements that can be considered independent of the restoration strategy, and that are relevant for the discussion on the origin of the Hallstatt units.

Triassic-Jurassic evolution of the central NCA: Allochthony scenario

In all sections, the allochthony scenario restores at Late Triassic times (Figs. 8d, 9d, 10d) to a configuration where the platform domains lie to the North (left on the sections). The Hallstatt units of the Lammertal, Altausee and Bad Mitterndorf Zones, and the allochthonous platform elements (Schwarzer Berg in Fig. 8d, Tauplitzalm unit in Fig. 10d) lie to the South, above thick Permo-Triassic evaporites. Extensional faults that offset the pre-Permian Austroalpine basement have been inferred to account for: a) an increase in Ladinian thickness in the Osterhorngruppe (Fig. 8d); b) a major thickening of the Ladinian to Norian carbonate platforms from the Langbathseen into the Höllengebirge (Fig. 9d); and c) thickening of the Ladinian from the Kasberg into the Totesgebirge (Fig. 10d). This interpretation is inconsistent with the post-rift nature of the Ladinian to Norian (Mandl 2000; Leitner and Spötl 2017; Strauss et al. 2021), but an alternative solution, consistent with the allochthony scenario, has not been found. Furthermore, and counterintuitively, in the case of Section 3, the Ladinian basin of the Kasberg developed above a basement high and its equivalent Totesgebirge platform developed above down-thrown basement (Fig. 10d).

On the three sections, emplacement of the allochthonous Hallstatt and Triassic platform units takes place in the Jurassic (Figs. 8c, 9c, 10c). The allochthonous units are represented as isolated, rootless units, as could be expected for gravitationally emplaced olistolith masses. This geometry could be interpreted differently if one were to assume the allochthonous units to be part of an accretionary prism or a fold-and-thrust system. The overall relationship with the underlying Triassic and the overlying Jurassic would, however, be the same.

Other than the allochthonous Hallstatt and platform units, the only other unit experiencing major displacement is the Totesgebirge-Kaseberg unit as it is thrusted over the Kasberg footwall (Fig. 10c, d). A Late Jurassic age of the

Kasberg thrust is based on its westward continuation as the Totesgebirge thrust to the southern limb of the Rettenbach valley (Tollmann 1976b). In the Rettenbach valley (transected on Section 2, Fig. 6), Middle to Upper Jurassic sediments onlap the growing Totesgebirge structure (Missoni and Gawlick 2011; Mandl 2013).

On all three sections, activity on faults displacing the pre-Permian basement is also inferred to occur during the Late Jurassic. On Section 1, significant uplift is inferred for the basement below the Tennegebirge unit to account for the lack of Upper Jurassic deposits. This basement uplift feeds the thrusting and uplift of the Trattberg Rise (Fig. 8c). The Trattberg Rise in turn acts as a backstop to the northward advance of the Schwarzer Berg-Sattleberg allochthonous units. On Section 2, basement faulting is inferred under the Rettenbach to account for the onlap of Upper Jurassic sediments onto the Upper Triassic of the Singereben unit (Mandl 2013) and under the Dachstein unit to account for the lack of widespread Upper Jurassic deposition in this area (Fig. 9c). On Section 3, basement uplift is inferred to have uplifted the Totesgebirge unit (Fig. 10c).

The restoration to the Late Jurassic of the sections for the allochthony scenario reveals a series of inconsistencies:

1) The reconstructed position of the allochthonous units of the Sattleberg and Schwarzer Berg on Section 1 indicates a very elevated position relative to the adjoining basins (Fig. 8c). Surprisingly, the Upper Jurassic basin of the Osterhorngruppe records no sediment supply from the allochthonous units of the Lammertal Zone, even though their emplacement, pre-dates the full development of the Trattberg Rise uplift and the Tauglboden basin (Gawlick et al. 2009). Likewise, Lower Cretaceous sediments in the area do not record sediments of a local provenance (Braun 1998), contrasting with the topographic prevalence of the Sattleberg-Schwarzer Berg units suggested by this scenario;
2) The Ramsau and Hoher Sarstein Jurassic, on Section 2 (Fig. 9c), cannot be accounted for satisfactorily in this model. The Ramsau Jurassic rests directly above Lower Triassic and Anisian rocks of the trailing edge of the Höllengebirge-Singereben unit, and is therefore restored to an anomalously deep position, despite it exhibiting reefal facies (Mandl et al. 2014). The Hoher Sarstein Jurassic, in turn, appears isolated from other Jurassic occurrences in spite of it containing reefal debris (Schlagintweit and Gawlick 2006); and
3) Although area balance is not the objective of the restoration, it is worth mentioning that Sections 2 and 3 present problems with respect to balance (Figs. 9c, d, 10d). On Section 3 this is possibly related to out-of-plane motion on the Kasberg thrust. On Section 2 the area balance problem is larger and stems from interpreting that the pre-Permian basement below the Dachstein unit is part of the Höllengebirge unit (and not of the Dachstein unit, as proposed in the autochthony scenario).

Triassic-Jurassic evolution of the central NCA: Autochthony scenario

The restoration to Late Triassic time of the autochthony scenario of the three sections (Figs. 8h, 9h, 10h) results in a paleogeography that strongly contrasts with that of the allochthony scenario. The structural units observed on the three sections (Figs. 5, 6, 7) are interpreted to have been in the same order of N-S relative arrangement at the end of the Triassic. The Hallstatt units of the Lammertal, Altaussee and Bad Mitterndorf Zones are interpreted to overlie salt diapirs that provided a substrate for these deep water domains (Figs. 8h, 9h, 10h).

As with the case of the allochthony scenario, extensional faults have been interpreted in the basement (Figs. 8h, 9h, 10h). However, unlike the allochthony scenario, changes in the thickness of the Middle to Late Triassic are interpreted to result from halokinetics. In this model, Triassic carbonate platforms developed as basins that subsided into the Permo-Triassic evaporites and were bounded by broad salt diapirs. Subsidence of these diapirs during growth (possibly led by extension, cf., Vendeville and Jackson 1992) generated the deep-water domains of the Hallstatt basin seaways. A similar model of Triassic carbonate basins floored by diapirs was proposed by Strauss et al. (2021) for the eastern NCA. Locally, however, the diapirs are also capped by relatively Middle to Upper Triassic carbonate platform successions (the Schwarzer Berg unit on Fig. 8h, the Kasberg and Tauplitzalm units on Fig. 10h). Partial collapse of the northern margin of the Dachstein platform above a thick Permo-Triassic evaporite body can account for the presence of Hallstatt limestone directly overlying the Norian platform carbonates on the Hoher Sarstein (Fig. 9h) and slump folding of the platform carbonates (Fernandez et al. 2022).

The autochthony scenario results in a significantly reduced amount of shortening expected on the sections, but still implies shortening in the order of up to a few tens of kilometers (Figs. 8g,h, 9g,h, 10g,h). The Permo-Triassic evaporite is interpreted to have facilitated the decoupling of the NCA from its basement and helped localize deformation during the Late Jurassic. It is here interpreted that contractional deformation concentrated in the platform-to-basin transitions as well as in the necking points of the carbonate platforms (e.g., the boundaries

between Osterhorngruppe and Schwarzer Berg, Fig. 8g, between the Totesgebirge and Tauplitzalm, Fig. 10g). The original thickness of the Permo-Triassic evaporites implied by the autochthony scenario, calculated by dividing the cross-sectional area of evaporites in the Triassic by the restored section length (Figs. 8h, 9h, 10h), is in the range of 700 to 1000 meters (in line with the estimates of Leitner and Spötl 2017).

Aside of a possible influence of the basement, squeezed salt diapirs are the main generators of uplift during Jurassic shortening. As a result, shallow-water Upper Jurassic reefs grew preferentially atop the squeezed diapirs of the Altaussee Zone, of the Ramsau, and of the Bad Mitterndorf Zone, a feature described by Tollmann (1981) and also observed by Kurz et al. (under review). The reef that crowned the Altaussee Zone would account for the Upper Jurassic perireefal facies of the Hoher Sarstein (Fig. 9g). Triassic diapirism (Fig. 9h) and shortening-related uplift can also provide an explanation for the omission of Middle Triassic platform carbonates below the Upper Jurassic reefs of the southern margin of the Dachstein unit. Furthermore, the more moderate uplift of the Schwarzer Berg in the autochthony scenario better accounts for the absence of sediments sourced from the Lammertal Zone in the Jurassic basin of the Osterhorngruppe (Gawlick et al. 2009) and in the Lower Cretaceous (Braun 1998).

Finally, the autochthony model implies that the Altaussee Zone thrust of Jurassic age (Fig. 9g) is the along-strike equivalent to the Totesgebirge thrust (of Tollmann 1976b) and the Kasberg thrust (Fig. 10g), whose Jurassic age has been discussed above.

Post-Jurassic tectonism: Both scenarios

The post-Jurassic structural evolution along the three cross-sections is similar in both the autochthony and allochthony scenarios. One of the main post-Jurassic tectonic events in the region is the emplacement of the Dachstein thrust sheet (Fig. 6). This thrust sheet overrides the Upper Jurassic sediments immediately west of Section 2 (Fernandez et al. 2022) and its leading edge is partly overlain by Lower Cretaceous sediments (Schäffer 1982). Lower Cretaceous breccias contain abundant clasts of Upper Jurassic age as well as clasts derived from the Hallstatt units (Krische and Gawlick 2015), indicating uplift and wasting in the Altaussee Zone. The absence of clasts derived from the Norian platform of Dachstein thrust sheet (Krische and Gawlick 2015) potentially implies that this thrust sheet had a more subdued relief than the neighboring Altaussee Zone during the Early Cretaceous, and mirrors the limited reworking of pre-thrusting units during Cretaceous thrusting in the western NCA. Thrusting on the Dachstein thrust continues into the Paleogene, tilting and overriding Upper Cretaceous sediments (Levi et al. 2022).

Besides within-NCA deformation, during the Cretaceous the NCA were thrusted northwards and were mostly decoupled from their pre-Permian basement along the Permo-Triassic evaporites and clastics. Ongoing shortening led to the NCA being thrust over the Penninic units (Figs. 8b, f, 9b, f, 10b, f). At least partly coeval with these events are the development of the Upper Cretaceous fault-bounded depocenters (Wagreich and Decker 2001; Fernandez et al. 2022), extensional faulting between the Osterhorngruppe and the Schwarzer Berg (Fig. 8b, f), and extension within the thrusted Dachstein unit (Fig. 9b, f) (Fernandez et al. 2022). Although some Cretaceous faulting is associated with transcurrence (Wagreich and Decker 2001), a possible link to salt-cored deformation (cf., Fernandez et al. 2022) has been incorporated in the autochthony scenario (Figs. 8f, 9f, 10f).

A subsequent and final phase of deformation is that relating to strike-slip motion between the different Triassic platform blocks of the NCA (Ratschbacher et al. 1991; Linzer et al. 1995; Peresson and Decker 1997). This event is represented on the cross-sections with the transport of the Mandlingzug onto the southern margin of the Dachstein (Fig. 9a, e) displacement on the KLT fault system (Figs. 8a, e, 9a, e). It is not the objective of this contribution to detail the deformation along this fault and associated splays, which has been covered in detail by other authors (e.g., Decker et al. 1994; Levi et al. 2022). In the restorations, displacement on this fault system has not been modelled, a simplification that does not affect the essence of the relationships between the different units during the key Jurassic and Triassic phases.

Discussion

Allochthony versus Relative autochthony: The role of salt tectonics in the NCA

The debate on the the allochthony or relative autochthony of the Hallstatt units in the central NCA extended over most of the 20th century. It was mostly brought to a close by the contribution of Tollmann (1981) in which he proposed a model for the gravitationally-driven emplacement of the Hallstatt units (*Gleittektonik*). This model was further elaborated by other authors and consolidated to its current understanding (Mandl 2000). Likewise, an

alternative mode of emplacement of the Hallstatt units, as part of a now dismembered accretionary prism, has been proposed (Gawlick et al. 1999; Missoni and Gawlick 2011; Gawlick and Missoni 2019).

Since the 1980s, with the consolidation around the hypothesis of an allochthonous derivation of the Hallstatt units, the possibility of an alternative interpretation has fallen into disregard. Recent research in the eastern and central NCA has, however, revealed the potential relevance of salt tectonics in the development of Triassic platforms in the NCA (Granado et al. 2019; Fernandez et al. 2021; Strauss et al. 2021; Kurz et al. under review). In the central NCA, the extensive presence of salt diapirs (Schauberger 1955; 1986) makes the question of the role of salt (as intra-platform diapirs or as allochthonous masses) all the more poignant. Modern concepts in salt tectonics, developed mostly since the late 1980s (Jackson and Hudec 2017) render a re-evaluation of the NCA under the perspective of halokinesis reasonable. Beyond the results from the section restoration presented above, we explore here the possible value of a new model for the NCA in which salt tectonics plays a prominent role.

For a start, salt tectonics can help explain the origin of stratal wedges observed at diverse locations within the Norian carbonate platforms of the central NCA (Fig. 11). At least two of these (Figs. 11a, c) are located in the immediate vicinity of known salt diapirs. These wedges can be interpreted as the result of thickening of the Norian carbonates away from growing diapiric structures, and into adjoining salt-bounded basins. Similar geometries are well known from other salt provinces (e.g., Kwanza basin, Fig. 12). At map scale, Tollmann (1960), Schöllnberger (1973), and Schmid et al (2003) also document thinning of the Norian platform carbonates from the Totesgebirge unit into the Tauplitzalm unit (Fig. 7c). Fernandez et al. (2022) documented the onlap (and thinning) of Norian platform carbonates onto underlying Ladinian platform carbonates in the hanging wall of the Dachstein thrust sheet. On a more local scale, Fernandez et al (2021; 2022) described growth geometries within Norian platform carbonates that support the idea of deposition above Permo-Triassic salt (as proposed by Schauberger 1955). Thickness changes in the NCA are not limited to Norian carbonates. Cornelius and Plöchinger (1953) and Häusler (1980) also document a major change in the thickness of the Anisian carbonates in the vicinity to Section 1, with thickness varying laterally over less than one kilometer from ~150 m to more than 600 m. A fault-related origin of these growth geometries would be at odds with the Anisian end of rifting, whereas they can be accounted for by post-rift halokinesis.

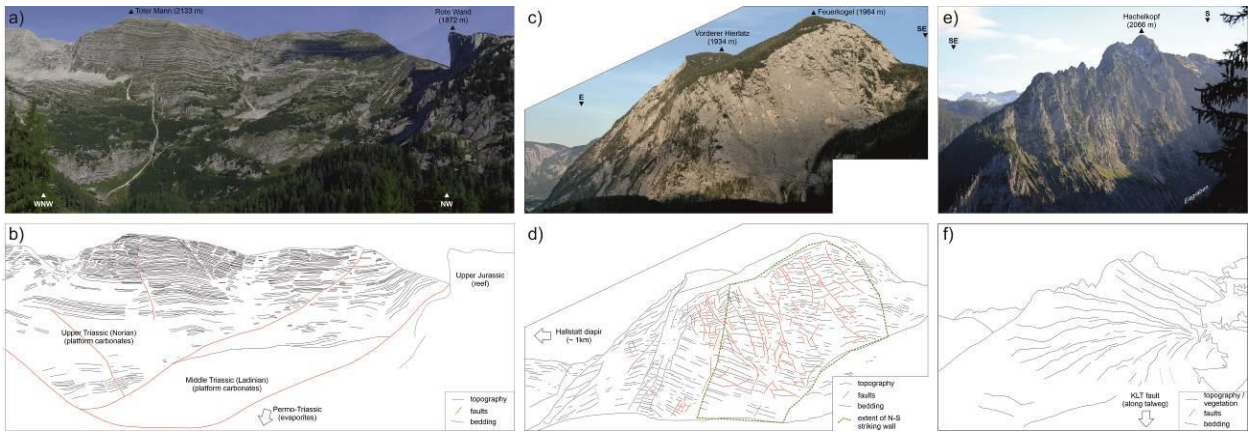

Fig. 11 Examples of growth wedges in Upper Triassic (Norian) lagoonal carbonates. See Fig. 3 for location. **a,b** Growth wedge in lagoonal Norian carbonates against a now collapsed diapir (location of Permo-Triassic outcrops). Modified from Kurz et al. (under review) **c,d** Growth wedge in lagoonal Upper Triassic (Norian) carbonates south of the Hallstatt diapir (Schorn and Neubauer 2014; Fernandez et al. 2021). The area marked by the dashed line indicates the segment of the wall that runs roughly N-S and on which geometries are not significantly distorted by perspective. **e,f** Growth wedge of lagoonal Upper Triassic (Norian) carbonates against the Königssee-Lammertal-Traunsee (KLT) fault. Wedging is only seen on the southern block of this fault and has not been documented to its north. Photo courtesy of Christian Schneider.

In addition, a thick basal evaporite unit can explain the structures of Jurassic-age observed in the central NCA. Most relevantly, the backthrusts of the Lammertal and Bad Mitterndorf Zone units onto the Tennengebirge and Grimming units (Figs. 5 and 7) are similar to the structure of the Gamstein unit farther east in the NCA (interpreted and modelled by Santolaria et al. 2022). Similar structures can also be observed above the thick Aptian salt of the southern Atlantic (Fig. 12a-c). The geometry of mini-basins E_1, E_2 and F in Fig. 12b is analogous to the structure on

Sections 1 and 3. On Section 1, mini-basin E_1 is analogous to the Osterhorngruppe unit, mini-basin E_2 is analogous to the Schwarzer Berg, and mini-basin F is analogous to the Tennengebirge unit (Fig. 5c). On Section 3, mini-basin E_1 is analogous to the Totesgebirge unit, mini-basin E_2 is analogous to the Tauplitzalm, and mini-basin F is analogous to the Grimming unit (Fig. 7c). On Section 3, the structure of mini-basin D above mini-basin C (Fig. 12b) is analogous to the structure of the Kasberg thrust (Fig. 7c).

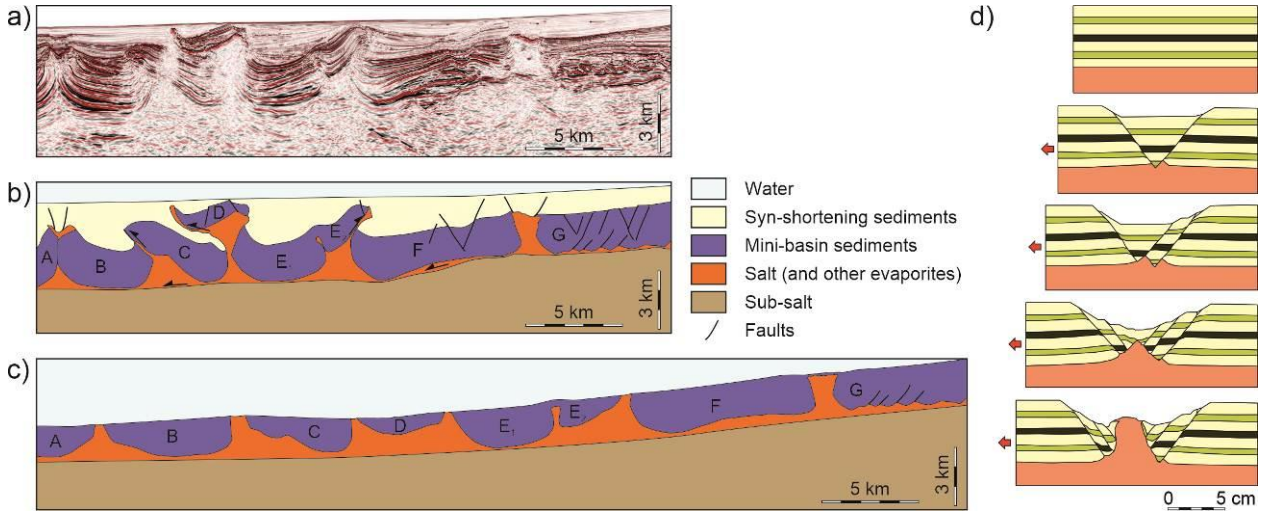

Fig. 12 a Reflection seismic profile migrated in depth, from the offshore Kwanza basin (Angola) (courtesy of Sonangol). Mini-basins above the salt have developed initially in passive down-building and subsequently have glided downslope, leading to shortening above the salt layer. **b** Interpretation of the seismic profile and identification of individual mini-basins. Sediments are separated into those deposited within the mini-basins during down-building, and sediments deposited during basinward gliding of the mini-basins due to tilting of the passive margin. **c** Reconstruction of the restored position of the mini-basins in **(b)** prior to down-slope gliding (gliding to the left). **d** Analogue sandbox model illustrating the negative relief above a diapir growing in extension. This model of growth could account for the presence of subsiding basins above salt structures within the Triassic shallow water carbonate platform. After Vendeville and Jackson (1992)

The salt-tectonics model presented here can also help to explain the observation of Kenter and Schlager (2009) who discuss the need of a "pedestal" beneath the Hallstatt units of the NCA. A "salt pedestal" has been invoked in Figs. 8h, 9h, and 10h, similar to the model proposed by Häusler (1980) and Strauss et al. (2021). Negative relief above a growing diapir is known to occur for diapirs growing under extension (reactive diapir growth; Fig. 12d; Vendeville and Jackson 1992) and could account for the deposition of the Hallstatt units in seaways within the NCA platform domain (similar to the paleogeographic model in Fig. 4c). The tectonic extension necessary for negative bathymetry diapirs could have been driven by downslope sliding of the NCA on the Triassic passive margin (similar to that observed in the southern Atlantic Cretaceous margin, Fig. 12b, c, and also proposed by Strauss et al. 2021 and Santolaria et al. 2022 for the eastern NCA). It is worth mentioning, that in contrast to the controversy surrounding the origin of the Hallstatt units, the accumulation of deep-water carbonate successions (Seefeld Fm) within the Norian platform domain of the Hauptdolomit in the western NCA has always been accepted (e.g., Brandner and Poleschinski 1986; Donofrio et al. 2003). The Hauptdolomit intraplatform basins may have been similarly related to a combination of extension and reactive diapir growth.

Over the central and eastern NCA, the widespread presence of Norian reefs along the northern fringe of the Hallstatt seaways (Zankl 1967, Tollmann 1981; Figs. 4c, d), but their absence along their southern fringes, may simply reflect the typical difference between the windward (reefs) and leeward (carbonate sand bodies, platform shoulders) margins (cf. Hine et al. 1981). The presence of Ladinian and Norian platform detritus in the deep-water units of the purported Hallstatt seaways (Pistotnik 1972; Galwick 1998; Hornung et al. 2007; Mette et al. 2019) proves the syn-depositional vicinity of these domains. Pistotnik (1974) placed the deposition of the Hallstatt carbonates within these same seaways, as they are observed to transit laterally into the platform slope facies. Notwithstanding, these observations may, in principle, also be explained within a "single platform – single Hallstatt facies belt" framework in combination with allochthonous emplacement.

As pointed out by several authors (e.g., Pistotnik 1974; Frisch and Gawlick 2003), however, and as contained in the cross-sections presented (Figs. 5-7), complete transitions from the Hallstatt units into the Norian platform successions are mostly strongly tectonized. A "smoking gun" observation in favor of these transitions into an intra-NCA seaway has not yet been made. The transition documented by Kenter and Schlager (2009) is traditionally assumed to represent the transition into the southern, distal deep-water Hallstatt domain of the Tollmann (1981) model, i.e., into the open Neotethys ocean. The lack of documented complete platform-to-basin transitions notwithstanding, the structural model presented here in favor of a relative autochthonous origin of the Hallstatt units represents a viable framework to identify areas for future investigation. Likewise, the tectonic evolution of the relative autochthony scenario (Figs. 8e-h, 9e-h, 10e-h) contains less internal inconsistencies than that of the allochthony scenario (Figs. 8a-d, 9a-d, 10a-d). We hold that the relative autochthony scenario poses no major difficulties that may detract from the validity of cross-sections, and clarifies the known distribution of Mesozoic depocenters and facies. In contrast, the allochthony model requires assumptions that are not fully consistent with the present understanding of the structural history of the central NCA (e.g., the need for extensional faulting into the Late Triassic) and fails to fully account for the evolution of the small, but critical outcrops of the Hoher Sarstein and Ramsau (Section 2; Fig. 9b-c).

Post-Triassic shortening and strike-slip

The possibility of a relative autochthonous origin of the Hallstatt units, as described above, brings back the debate, already raised by Zankl (1967), on the internal shortening of the NCA. Zankl (1967), comparing his work with that of Spengler (1956), stated that shortening with a scenario of relative autochthony of the Hallstatt units would yield ~50% the shortening of a scenario of allochthony. Our restorations, assuming that out-of-plane motion similarly affects both scenarios, indicate that shortening is 20-50% smaller in relative the autochthony scenario (Figs. 8-10).

Another aspect of post-Triassic deformation not specifically addressed in the restorations is the role of Neogene strike-slip tectonics. As discussed above, the most relevant effect of strike-slip observable on the cross-sections is the juxtaposition of the Mandlingzug against the southern end of the Dachstein unit (Fig. 9). The absence of a well-developed Norian succession (Figs. 6, 9) has led previous authors to propose that the Mandlingzug is allochthonous (e.g., Frisch and Gawlick 2003). However, a similar stratigraphic arrangement (a condensed Norian) has been documented by Santolaria et al (2022) for the Hochschwab unit in the eastern NCA. These authors have explained this feature as the result of drowning of the distal platform unit due to salt-driven down-slop sliding. This mechanism has not been explored here, but could provide a reasonable explanation.

The other major strike-slip structure that cross-cuts the area is the KLT fault system (Decker et al. 1994; Levi et al. 2022). As shown in Fig. 11e, growth strata in the Norian platform succession adjacent to this fault suggests a Triassic origin for this structure, at least in its Königssee segment. The frequent exposure of Permo-Triassic evaporites and Lower Triassic rocks along the trace of the fault system farther to the east (Decker et al. 1994; Levi et al. 2022) might indicate that the structure developed initially as a salt-cored structure. If this observation is correct, it could imply that the KLT and other Neogene strike-slip fault corridors developed along pre-existing Triassic salt structures (likely squeezed during the Jurassic and Cretaceous). Such a scenario might require a re-evaluation of the amount of Neogene displacement, to remove the potential effect of inherited offset related to earlier phases of activity.

Metamorphism

A final constraint on the tectonic evolution of the NCA that has not been fully explored are data on metamorphism. In the central NCA, metamorphic crystallization ages are consistently Cretaceous (Kralik et al. 1987; Frank and Schlager 2006). Metamorphic grade generally increases towards the southern edge of the NCA, and downwards to the Austroalpine basement, with anchimetamorphic to epimetamorphic grade reached in Permo-Triassic rocks south of the Tennengebirge. It can be inferred from this, that during the Cretaceous the trailing edge of the NCA was tectonically buried below units that have since been eroded. Some of these units might have comprised NCA-style stratigraphy, which would imply a wider southward extent of the Triassic NCA platform-and-basin domain. This would further imply that the Norian platform-basin transition of the Gosaukamm (Kenter and Schlager 2009) may have, in fact, been facing an intraplatform seaways.

Record of anchi- to epimetamorphism also appears, patchily, in locations farther north, in the Lammertal Zone and in the Bad Reichenhall area (Kralik et al. 1987; Frank and Schlager 2006) (Fig. 13). These areas are not expected to have been buried significantly in the Cretaceous (see Fig. 8b, c for the Lammertal Zone). Kralik et al. (1987) argue in favor of a shallow origin for the anchi- to epimetamorphic signal, as would be suggested by apatite fission-track

data that supports temperatures below 100°C since the Early Cretaceous (Heijl and Grundmann 1989). Alternative interpretations have not been found, and the question remains open for both the allochthony and autochthony scenarios.

Implications for the structure of the central NCA

Thrust system subdivision

The cross-sections and restorations presented herein raise issues with respect to the traditional subdivision of the NCA. Section 2 (Fig. 6) is the most complete one and cuts across the three thrust systems historically defined in the NCA: the Bajuvaric, Tirolic and Juvavic systems. On Section 2 (Fig. 6b, c): a) the Bajuvaric system corresponds to the Langbathseen unit; b) the Tirolic system encompasses the Höllengebirge and Singereben units along with their southern prolongation all the way to under the Dachstein thrust sheet; and c) the Juvavic system is represented by the Dachstein thrust sheet and the Altaussee Zone (only valid for Fig. 6b). The boundary between the Bajuvaric and Tirolic systems is the Höllengebirge thrust (Fig. 13) and between the Tirolic and Juvavic systems is the Dachstein thrust (Fig. 13). The restoration of Section 2 (Fig. 9d, h), highlights the contrast in stratigraphic thickness from the Bajuvaric to the Tirolic system (from the Lanbathseen to the Höllengebirge unit). However, hardly any difference is observed between the Tirolic and Juvavic systems (between the Singereben and Dachstein units) (Fig. 9d, h). The Dachstein thrust can therefore proposed here to be an internal thrust of the Tirolic system (ultra-Tirolic of Frisch and Gawlick 2003). Furthermore, it is proposed that the Dachstein thrust extends eastward, between the Totesgebirge and the Grimming-Warscheneck block (along the Tauplitzalm, Fig. 7) to the Windischgarsten Zone (Fig. 13). The direction of emplacement of the Dachstein thrust sheet has not been determined, but a northeast-directed transport would be consistent with kinematic criteria recorded by Decker et al. (1994) and with the role of the Osterhorngruppe-Gamsfeld and Totesgebirge-Warscheneck boundaries (Rigaus and Salzsteigstörung of Decker et al. 1994) as lateral ramps (Fig. 13).

Jurassic structural framework

Jurassic structures comprise two main belts. A northern belt is formed by the north- to northeast-trending Totesgebirge thrust and Trattberg Rise (a trend partly overthrust by the Dachstein thrust sheet) (Fig. 13). The Totesgebirge-Trattberg structure, which involves the entire Triassic succession of the Osterhorngruppe and Totesgebirge units, correlates with the thrust at the base of the Altaussee Zone in the autochthony scenario. The southern belt of Jurassic structures corresponds to the northward-dipping basal contact of the Lammertal and Bad Mitterndorf Zones, juxtaposing Hallstatt units on Triassic platform carbonates. These contacts are laterally continuous and named here the Sattelberg and Mitterndorf thrusts (Fig. 13). In the allochthony scenario, these are north-directed thrusts, whereas in the autochthony scenario, they are south-directed backthrusts. This southern belt also includes the Jurassic contacts of the Hallstatt diapir and the Wurzeralm contact (Fig. 13). Both contacts have been interpreted as the result of contractional salt tectonics (Fernandez et al. 2021; Kurz et al. under review).

Open questions

Other than the aspects that need to be further explored to test the alternative scenarios for the stratigraphic and structural development of the NCA, there are number of more general questions that arise from the work presented herein, namely:

1) What is the direction of tectonic shortening within the central NCA during the Jurassic shortening phase? What is the relationship (if any) between the northern and southern trends of Jurassic structures? What was the role of the Austroalpine basement during this phase?
2) What was the direction of Early Cretaceous thrusting?
3) Tollmann (1964) already concluded that the definition of thrust sheets based exclusively on criteria related to facies is only partly applicable in the eastern NCA. If the scenario of relative autochthony of the Hallstatt units were proven to be valid, facies-based structural subdivision of the central NCA would require a major revision. Is it possible that the historical, facies-based approach could be unduly influencing the interpretation of the structure and evolution of the NCA in broader terms?

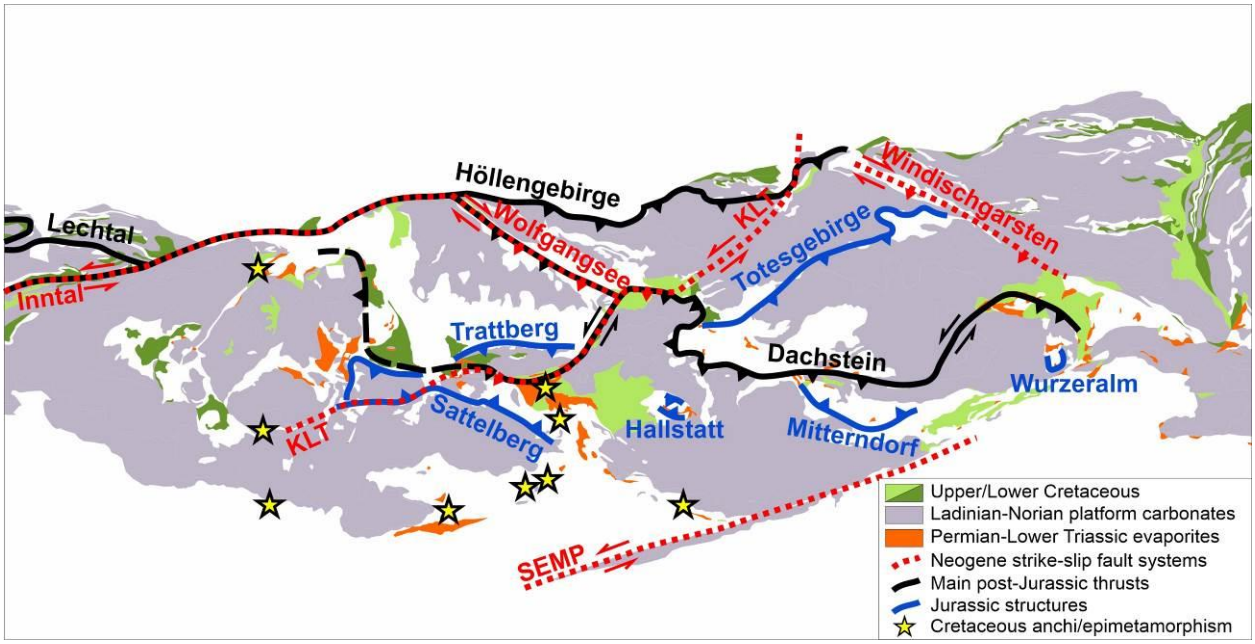

Fig. 13. Simplified map of the central NCA showing the main structures in the region. The Höllengebirge thrust (of Cretaceous age) separates the Tirolic thrust system from the Bajuvaric thrust system. The Dachstein thrust (of Cretaceous age) was previously used to separate the Juvavic from the Tirolic units, but is here considered part of the Tirolic thrusts. Its western prolongation into the Berchtesgaden area is uncertain. The Trattberg Rise and Totesgebirge thrust (of Jurassic age) have been partly overridden by the Dachstein thrust sheet. The Sattlberg, Mitterndorf, Hallstatt and Wurzeralm structures are Jurassic contacts juxtaposing Hallstatt deep water carbonates on Triassic platform units. Sites of Cretaceous anchi- or epimetamorphism from Kralik et al. 1987. At: Altaussee; Bg: Berchtesgaden; BM: Bad Mitterndorf; BR: Bad Reichenhall; Da: Dachstein; Ga: Gamsfeld; Go: Gosau; Gr: Grimming; HG: Hoher Göll; Hö: Höllengebirge; Ka: Kasberg; Lm: Lammertal; Mg: NCA southern margin; Mz: Mandlingzug; Oh: Osterhorngruppe; SB: Schwarzer Berg; Si: Singereben; Tn: Tennengebirge; Tt: Totes Gebirge; Ub: Untersberg; Uk: Unken; Wi: Windischgarsten Wk: Warscheneck

Conclusion: One geology, two interpretations

The cross-sections and restorations shown in this contribution aim to re-cast the debate on the origin of the Hallstatt units with from a modern structural geological perspective. Two alternative, and strongly contrasting scenarios are presented by means of cross-sections constrained by data from wellbores and outcrops. A scenario of allochthony of the Hallstatt units is based on the assumption that the Triassic facies belts along the NCA passive margin graded laterally from a single shallow-water platform in the North (Hauptdolomit-Dachsteinkalk megabank) into a single deep-water Hallstatt basin in the South. During the Middle to Late Jurassic, the basinal Hallstatt units were subject to northward long-distance transport, either by gravitational sliding or incorporated in an accretionary prism. A scenario of relative autochthony of the Hallstatt units is based on the assumption of Triassic salt tectonism in the central NCA, with the Hallstatt units deposited in subsiding, salt-floored seaways between partially isolated Triassic carbonate platforms.

The restoration of these alternative scenarios highlights inconsistencies of structural evolution implied by the scenario of allochthony, and points out the key aspects that need to be addressed to better support scenario of relative autochthony based on salt tectonics.

Irrespective of the validity of each scenario, the sections and restorations presented here raise major questions about the traditional structural subdivision of the central NCA, and provides a modern structural framework within which to conduct future research.

References

Baumgartner P (2013) Mesozoic radiolarites – accumulation as a function of sea surface fertility on Tethyan margins and in ocean basins. Sedimentology 60:292-318. https://doi.org/10.1111/sed.12022

Bechstädt T, Schweizer T (1991) The carbonate-clastic cycles of the East-Alpine Raibl group: result of third-order sea-level fluctuations in the Carnian. Sed Geol 70:241-270.

Brandner R, Poleschinski W (1986) Stratigraphie und Tektonik am Kalkalpensüdrand zwischen Zirl und Seefeld in Tirol (Exkursion D am 3. April 1986). Jahresberichte und Mitteilungen des Oberrheinischen Geologischen Vereines, Neue Folge 68:67-92.

Braun R (1998) Die Geologie des Hohen Gölls. Nationalpark Berchtesgaden Forschungsbericht 40/1998, Berchtesgaden.

Brix F, Schultz O (1993) Erdöl und Erdgas in Österreich. Naturhistorisches Museum Wien, Vienna.

Brückl E, Bleibinhaus F, Gosar A, Grad M, Guterch A, Hrubcová P, Keller GR, Majdański M, Šumanovac F, Tiira T, Yliniemi J, Hegedűs E, Thybo H (2007) Crustal structure due to collisional and escape tectonics in the Eastern Alps region based on profiles Alp01 and Alp02 from the ALP 2002 seismic experiment. J Geophys Res 112:B06308. https://doi.org/10.1029/2006JB004687

Cornelius HP, Plöchinger B (1952) Der Tennengebirgs-N-Rand mit seinen Manganerzen und die Berge im Bereich des Lammertales. Jahrb Geol Bundesanst 95:145-225.

Decker K, Peresson H, Faupl P (1994) Die miozäne Tektonik der östlichen Kalkalpen: Kinematic, Paläospannungen und Deformationsaufteilung während der “lateralen Extrusion” der Zentralalpen. Jahrb Geol Bundesanst 137:5-18.

Donofrio D, Brandner R, Poleschinski W (2003) Conodonten der Seefeld-Formation: Ein Beitrag zur Bio- und Lithostratigraphie der Hauptdolomit-Plattform (Obertrias, westliche Nördliche Kalkalpen, Tirol). Geologisch-Paläontologische Mitteilungen Innsbruck 26:91-107.

Egger H (1996) Geologische Karte der Republik Österreich 1:50,000 Blatt 66 Gmunden. Verlag der Geologischen Bundesanstalt, Vienna.

Egger H, Briguglio A, Rögl F (2017) Eocene straigraphy of the Reichenhall basin (Eastern Alps, Austria, Germany). Newsletters on Stratigraphy 50:341-362. https://doi.org/10.1127/nos/2016/0333

Egger H, Heinrich M, van Husen D, Lobitzer H, Moshammer B, Pavuza R, Rupp C, Schedl A, Schubert G, Schuster R, Stummer G, Wagner L, Wessely G (2009) Erläuterungen zu Blatt 67 Grünau im Almtal. Verlag der Geologischen Bundesanstalt, Vienna.

Egger H, van Husen D (2003) Geologische Karte der Republik Österreich 1:50,000 Blatt 64 Strasswalchen. Geologische Bundesanstalt, Vienna.

Egger H, van Husen D (2007) Geologische Karte der Republik Österreich 1:50,000 Blatt 67 Grünau. Geologische Bundesanstalt, Vienna.

Faupl P, Wagreich M (2000) Late Jurassic to Eocene paleogeography and geodynamic evolution of the Eastern Alps. Mitt Österr Geol Ges 92:79-94.

Fernandez O, Grasemann B, Sanders D (2022) Deformation of the Dachstein Limestone in the Dachstein thrust sheet (Eastern Alps, Austria). AJES 115:167-190. https://doi.org/10.17738/ajes.2022.0008

Fernandez O, Habermüller M, Grasemann B (2021) Hooked on salt: Rethinking Alpine tectonics in Hallstatt (Eastern Alps, Austria). Geology 49:325-329. https://doi.org/10.1130/G47981.1

Frank W, Schlager W (2006) Jurassic strike slip versus subduction in the Eastern Alps. Int J Earth Sci 95:431-450. https://doi.org/ 10.1007/s00531-005-0045-7

921 Frisch W, Gawlick HJ (2003) The nappe structure of the central Northern Calcareous Alps and its disintegration
922 during Miocene tectonic extrusion— a contribution to understanding the orogenic evolution of the Eastern Alps. Int
923 J Earth Sci 92:712-727. https://doi.org/10.1007/s00531-003-0357-4

924 Frisch W, Kuhlemann J, Dunkl I, Brügel A (1998) Palinspastic reconstruction and topographic evolution of the
925 Eastern Alps during the late Tertiary tectonic extrusion. Tectonophysics 297:1-15.

926 Froitzheim N, Plašienka D, Schuster R (2008) Alpine tectonics of the Alps and Western Carpathians. In: McCann T
927 (ed) The Geology of Central Europe: Volume 2: Mesozoic and Cenozoic. Geological Society, London, pp 1141–
928 1232.

929 Gawlick H-J (1998) Obertriassische Brekzienbildung und Schollengleitung im Zlambachfaziesraum
930 (Pötschenschichten) – Stratigraphie, Paläogeographie und diagenetische Überprägung des Lammeregg-
931 Schollenkomplexes (Nördliche Kalkalpen, Salzburg). Jahrb Geol Bundesanst 141:147-165.

932 Gawlick H-J, Frisch W, Vecsei A, Steiger T, Böhm F (1999) The change from rifting to thrusting in the Northern
933 Calcareous Alps as recorded in Jurassic sediments. Geol Rundsch 87:644-657.

934 Gawlick H-J, Missoni S (2015) Middle Triassic radiolarite pebbles in the Middle Jurassic Hallstatt Mélange of the
935 Eastern Alps: implications for Triassic–Jurassic geodynamic and paleogeographic reconstructions of the western
936 Tethyan realm. Facies 61:13. https://doi.org/10.1007/s10347-015-0439-3

937 Gawlick H-J, Missoni S (2019) Middle-Late Jurassic sedimentary mélange formation related to ophiolite obduction
938 in the Alpine-Carpathian-Dinaridic Mountain Range. Gondwana Research 74:144-172.
939 https://doi.org/10.1016/j.gr.2019.03.003

940 Gawlick H-J, Missoni S, Schlagintweit F, Suzuki H, Frisch W, Krystyn L, Blau J, Lein R (2009) Jurassic
941 tectonostratigraphy of the Austroalpine Domain. Jour Alpine Geol 50:1-152.

942 Granado P, Roca E, Strauss P, Pelz K, Muñoz JA (2019) Structural styles in fold-and-thrust belts involving early salt
943 structures: The Northern Calcareous Alps (Austria). Geology 47:51-54. https://doi .org/10.1130/G45281.1.

944 Griffiths P, Jones S, Salter N, Schaefer F, Osfield R, Reiser H (2002) A new technique for 3-D flexural-slip
945 restoration. Jour Struc Geol 24:773-782.

946 Haas J, Kovács S, Krystyn L, Lein R (1995) Significance of Late Permian-Triassic facies zones in terrane
947 reconstructions in the Alpine-North Pannonian domain. Tectonophysics 242:19-40.

948 Hahn FF (1913a) Grundzüge des Baues der nördlichen Kalkalpen zwischen Inn und Enns, I. Teil. Mitt Österr Geol
949 Ges 9:238-357.

950 Hahn FF (1913b) Grundzüge des Baues der nördlichen Kalkalpen zwischen Inn und Enns, II. Teil. Mitt Österr Geol
951 Ges 9:374-500.

952 Hamilton W (1989) Geologische Ergebnisse von Tiefbohrungen im Flysch und Kalkalpin zwischen Wien und
953 Salzburg: Exkursionsführer der Österreichischen Geologischen Gesellschaft Nr 12. Österreichische Geologische
954 Gesellschaft, Vienna.

955 Häusler H (1980) Zur tektonischen Gliederung der Lammer-Hallstätter Zone zwischen Golling und Abtenau
956 (Salzburg). Mitt Österr Geol Ges 71/72:403-413.

957 Häusler H, Berg D (1980) Neues zur Stratigraphie und Tektonik der Hallstätter Zone am Westrand der
958 Berchtesgadener Masse. Verh Geol B-A 1980:63-95.

959 Heijl E, Grundmann G (1989) Apatit-Spaltspurdaten zur thermischen Geschichte der Nördlichen Kalkalpen, der
960 Flysch- und Molassezone. Jahresb Geol Bundesanst 132:191-212.

961 Hine A, Wilber R, Neumann A (1981) Carbonate sand bodies along contrasting shallow bank margins facing open
962 seaways in northern Bahamas. AAPG Bull 65:261-290.

Hornung T, Spatzenegger A, Joachimski MM (2007) Multistratigraphy of condensed ammonoid beds of the Rappoltstein (Berchtesgaden, southern Germany): unravelling palaeoenvironmental conditions on 'Hallstatt deep swells' during the Reingraben Event (Late Lower Carnian). Facies 53:267-292.

Jackson MPA, Hudec MR (2017) Salt Tectonics: Principles and Practice. Cambridge Univ Press, Cambridge.

Kenter JAM, Schalger W (2009) Slope angle and basin depth of the Triassic platform-basin transition at the Gosaukamm, Austria. AJES 102:15-22.

Kralik M, Krumm H, Schramm JM (1987). Low grade and very low grade metamorphism in the Northern Calcareous Alps and in the Greywacke Zone: Illite-crystallinity data and isotopic ages. In: Flügel HW, Faupl P (eds) Geodynamics of the Eastern Alps. Franz Deuticke, Vienna, pp 164-178

Krenmayr HG (2005) Geologische Karte von Salzburg 1:200,000. Geologische Bundesanstalt, Vienna.

Krenmayr HG (2013) Geologische Karte der Republik Österreich 1:50,000 Blatt 125 Bischofshofen. Geologische Bundesanstalt, Vienna.

Krenmayr HG, Schnabel H-J (2006) Geologische Karte von Oberösterreich 1:200,000. Geologische Bundesanstalt, Vienna.

Kreuss O (2020) Zusammenstellung ausgewählter Archivunterlagen der Geologischen Bundesanstalt GEOFAST 1:50,000 Blatt 128 Gröbming. Geologische Bundesanstalt, Vienna.

Krische O, Gawlick H-J (2015) Age and significance of Lower Cretaceous mass flows: Ischl Breccia revisited (Rossfeld Formation, Northern Calcareous Alps, Austria). AJES 108:128-150. https://doi.org/10.17738/ajes.2015.0017

Kurz M, Fernandez O, Eggerth L, Grasemann B, Strauss P (under review) Emplacement and associated sedimentary record of the Jurassic submarine salt allochthon of the Wurzeralm (Eastern Alps, Austria). Terra Nova.

Leitner C, Spötl C (2017) The eastern Alps: Multistage development of extremely deformed evaporites. In: Soto JI, Flinch JF, Tari G (eds) Permo-Triassic salt provinces of Europe, North Africa and the Atlantic margins. Tectonics and hydrocarbon potential. Elsevier, Amsterdam, pp 467-482. https://doi.org/10.1016/B978-0-12-809417-4.00022-7

Levi N, Pittarello L, Habermüller M (2022) Structural characteristics of the curved Königsee-Lammertal-Traunsee fault system in Salzkammergut (Northern Calcareous Alps, Austria). Jour Struc Geol 155:104503. https://doi.org/10.1016/j.jsg.2021.104503

Lingrey S, Vidal-Royo O (2015) Evaluating the quality of bed length and area balance in 2D structural restorations. Interpretation 3:SAA133-SAA160. https://doi.org/10.1190/INT-2015-0126.1

Linzer H-G, Decker K, Peresson H, Dell'Mour R, Frisch W (2002) Balancing lateral orogenic float of the Eastern Alps. Tectonophysics 354:211-237.

Linzer H-G, Ratschbacher L, Frisch W (1995) Transpressional collision structures in the upper crust: the fold-thrust belt of the Northern Calcareous Alps. Tectonophysics 242:41-61.

Mandl GW (1998) Geologische Karte der Dachsteinregion 1:50,000. Geologische Bundesanstalt, Vienna.

Mandl GW (2000) The Alpine sector of the Tethyan shelf – Examples of Triassic to Jurassic sedimentation and deformation from the North Calcareous Alps. Mitt Österr Geol Ges 92:61-77.

Mandl GW (2003) Hallstätter Kalke auf dem Sarstein? (Salzkammergut, Oberösterreich). Jahrb Geol Bundesanst 143:213–220.

Mandl GW (2013) Zur Geologie des Raumes Hütteneckalm–Sandlingalm–Blaa-Alm (Salzkammergut, Österreich) mit kritischen Anmerkungen zur Sandlingalm-Formation. Jahrb Geol Bundesanst 153:33-74.

Mandl GW, Hejl E, van Husen D (2014) Erläuterung zu Blatt 127 Schladming. Verlag der Geologischen Bundesanstalt, Vienna.

Mandl GW, van Husen D, Lobitzer H (2012) Erläuterung zu Blatt 96 Bad Ischl. Verlag der Geologischen Bundesanstalt, Vienna.

Mandl GW, Matura A (1995) Geologische Karte der Republik Österreich 1:50,000 Blatt 127 Schladming. Verlag der Geologischen Bundesanstalt, Vienna.

Mette W, Clemence M-E, Thibault N, Korte C, Konrad B, Ullman CV (2019) Sedimentology, carbon isotope stratigraphy and micropalaeontology of the Rhaetian Zlambach Formation– Implications for the Dachstein carbonate platform development (Northern Calcareous Alps, Austria). Sed Geol 382:47-60. https://doi.org/10.1016/j.sedgeo.2018.12.009

Miller C, Thöni W (1997) Eo-Alpine eclogitisation of Permian MORB-type gabbros in the Koralpe (Eastern Alps, Austria): new geochronological, geochemical and petrological data. Chem Geol 137:283-310.

Missoni S, Gawlick H-J (2011) Evidence for Jurassic subduction from the Northern Calcareous Alps (Berchtesgaden; Austroalpine, Germany). Int J Earth Sci 100:1605-1631. https://doi.org/10.1007/s00531-010-0552-z

Moser M (2014) Zusammenstellung ausgewählter Archivunterlagen der Geologischen Bundesanstalt GEOFAST 1:50,000 Blatt 97 Bad Mitterndorf. Geologische Bundesanstalt, Vienna.

Moser M, Pavlik W (2013) Zusammenstellung ausgewählter Archivunterlagen der Geologischen Bundesanstalt GEOFAST 1:50,000 Blatt 98 Liezen. Geologische Bundesanstalt, Vienna.

Ogg J (2015) The mysterious mid-Carnian "Wet Intermezzo" global event. Jour Earth Sci 26:181-191. https://doi.org/10.1007/s12583-015-0527-x

Ortner H (2003) Cretaceous thrusting in the western part of the Northern Calcareous Alps (Austria) – evidences from synorogenic sedimentation and structural data. Mitt Österr Geol Ges 94:63-77.

Ortner H (2017) Geometry of growth strata in wrench-dominated transpression: 3D-model of the Upper Jurassic Trattberg rise, Northern Calcareous Alps, Austria. Geophysical Research Abstracts 19:EGU2017-9222.

Ortner H, Ganser C, Stipp M, Fernandez O (2022) Deformation of a mountain-sized olistolith: Schwarzer Berg, Northern Calcareous Alps of Salzburg. Berichte der Geologischen Bundesanstalt 143:134.

Ortner H, Gaupp R (2007) Synorogenic sediments of the western Northern Calcareous Alps. Geo Alp 4:133-148.

Ortner H, Kilian S (2022) Thrust tectonics in the Wetterstein and Mieming mountains, and a new tectonic subdivision of the Northern Calcareous Alps of Western Austria and Southern Germany. Int J Earth Sci 11:543-571. https://doi.org/10.1007/s00531-021-02128-3

Ortner H, Stingl V (2001) Facies and basin development of the Oligocene of the Lower Inn Valley, Tyrol/Bavaria. In: Piller W, Raser M (eds) Paleogene in Austria. Schriftenreihe der Erdwissenschaftlichen Komissionen 14, ÖAW, Vienna, pp 153-196.

Ortner H, Ustaszewski M, Rittner M (2008) Late Jurassic tectonics and sedimentation: breccias in the Unken syncline, central Northern Calcareous Alps. Swiss J Geosci 101:S55-S71. https://doi.org/10.1007/s00015-008-1282-0

Pavlik W (2007) Provisorische Geologische Karte der Republik Österreich GEOFAST 1:50,000 Blatt 92 Lofer. Geologische Bundesanstalt, Vienna

Pavlik W (2009) Zusammenstellung ausgewählter Archivunterlagen der Geologischen Bundesanstalt GEOFAST 1:50,000 Blatt 93 Bad Reichenhall. Geologische Bundesanstalt, Vienna

Pavlik W (2013a) Zusammenstellung ausgewählter Archivunterlagen der Geologischen Bundesanstalt GEOFAST 1:50,000 Blatt 124 Saalfelden a. Stein. Meer. Geologische Bundesanstalt, Vienna

Pavlik W (2013b) Zusammenstellung ausgewählter Archivunterlagen der Geologischen Bundesanstalt GEOFAST 1:50,000 Blatt 125 Bischofshofen. Geologische Bundesanstalt, Vienna

Pavlik W (2014) Zusammenstellung ausgewählter Archivunterlagen der Geologischen Bundesanstalt GEOFAST 1:50,000 Blatt 98 Liezen. Geologische Bundesanstalt, Vienna

Peresson H, Decker K (1997) The Teriary dynamics of the northeastern Eastern Alps (Austria): changing paleostresses in a collisional plate boundary. Tectonophysics 272:125-157. https://doi.org/10.1016/S0040-1951(96)00255-7

Pistotnik U (1972) Zur Mikrofazies und Paläogeographie der Zlambachschichten (O. Nor - ? U. Lias) im Raume Bad Goisern – Bad Aussee (Nördliche Kalkalpen). Mitt Ges Geol Bergbaustud 21:279-288.

Pistotnik U (1974) Fazies und Tektonik der Hallstätter Zone von Bad Ischl – Bad Aussee (Salzkammergut, Österreich). Mitt Geol Ges Wien 66-67:143-158.

Plöchinger B (1964) Die tektonischen Fenster von St. Gilgen und Strobl am Wolfgangsee (Salzburg, Oberösterreich). Jahrb Geol Bundesanst 107:11-69.

Plöchinger B (1982) Geologische Karte der Republik Österreich 1:50,000 Blatt 95 Sankt Wolfgang. Geologische Bundesanstalt, Vienna.

Plöchinger B (1987) Geologische Karte der Republik Österreich 1:50,000 Blatt 94 Hallein. Geologische Bundesanstalt, Vienna.

Plöchinger B, Draxler I (1974) Gravitativ transportiertes permishes Haselgebirge in den Oberalmer Schichten (Tithonium, Salzburg). Verh Geol B-A 1974:71-88.

Ratschbacher L, Frisch L, Linzer H-G (1991) Lateral extrusion in the Eastern Alps, Part 2: Structural analysis. Tectonics 10:257-271.

Santolaria P, Granado P, Wilson E, de Matteis M, Ferrer O, Strauss P, Pelz K, König M, Oteleanu AE, Roca E, Muñoz JA (2022) From salt-bearing rifted margins to fold-and-thrust belts. Insights from analog modeling and Northern Calcareous Alps case study. Tectonics 41:e2022TC007503. https://doi.org/10.1029/2022TC007503

Schäffer G (1982) Geologische Karte der Republik Österreich 1:50,000 Blatt 96 Bad Ischl. Verlag der Geologischen Bundesanstalt, Vienna.

Schauberger O (1955) Zur Genese des alpinen Haselgebirges. Zeitschrift der deutschen Geologischen Gesellschaft 105:736-751.

Schlager W (1967) Hallstätter und Dachsteinkalk-Fazies am Gosaukamm und die Vorstellung ortsgebundener Hallstätter Zonen in den Ostalpen. Verh Geol B-A 1967:50-70.

Schlager W (1969) Das Zusammenwirken von Sedimentation und Bruchtektonik in den triadischen Hallstätterkalken der Ostalpen. Geol Rund 59:289-308.

Schlagintweit F, Gawlick H-J (2006) Sarstenia babai n.gen., n. sp., a new problematic sponge (inozoa?) from the Late Jurassic of the Northern Calcareous Alps, Austria. Rivista Italiana di Paleontologia e Stratigrafia 112:251–260.

Schmid C, Mandl GW, Wessely G (2003) Thermalwasserbohrung Bad Mitterndorf TH 1: Ein kalkalpiner tiefenaufschluss im steirischen salzkammergut. Gmunder Geo-Studien 2:255-264

Schmid SM, Bernoulli D, Fügenschuh B, Matenco L, Schefer S, Schuster R, Tischler M, Ustaszewski K (2008) The Alpine-Carpathian-Dinaridic orogenic system: correlation and evolution of tectonic units. Swiss J Geosci 101:139-183. https://doi.org/10.1007/s00015-008-1247-3

Schöllnberger W (1973) Zur Verzahnung von Dachsteinkalk-Fazies und Hallstätter Fazies am Südrand des Toten Gebirges (Nördliche Kalkalpen, Österreich). Mitt Ges Geol Bergbaustud 22:95-153.

Schorn A, Neubauer F (2014) The structure of the Hallstatt evaporite body (Northern Calcareous Alps, Austria): A compressive diapir superposed by strike-slip shear? Jour Struc Geol 60:70-84. http://doi.org/10.1016/j.jsg.2013.12.008

Schuster R, Egger H, Krenmayr HG, Linner M, Mandl GW, Matura A, Nowotny A, Pascher G, Pestal G, Pistotnik J, Rockenschaub M, Schnabel W (2015) Geologische Übersichtskarte der Republik Österreich 1:1,500,000 (Ohne Quartär). Geologische Bundesanstalt, Vienna.

Schuster R, Daurer A, Krenmayr H-G, Linner M, Mandl GW, Pestal G, Reitner JM (2019) Rocky Austria: Geologie von Österreich - kurz und bunt. Geologische Bundesanstalt, Vienna

Schweigl J, Neubauer F (1997) Structural evolution of the central Northern Calcareous Alps: Significance of the Jurassic to Tertiary geodynamics of the Alps. Eclogae geol Helv 90:303-323.

Spengler E (1956) Versuch einer Reokonstruktion des Ablagerungsraumes der Decken der Nördlichen Kalkalpen, II. Teil: Der Mittelabschnitt der Kalkalpen. Jarhb Geol Bundesanst 99:1-74.

Strauss P, Granado P, Muñoz JA (2021) Subsidence analysis of salt tectonics-driven carbonate minibasins (Northern Calcareous Alps, Austria). Bas Res 33:968-990. https://doi.org/10.1111/bre.12500

Stüwe K, Schuster R (2010) Initiation of subduction in the Alps: Continent or ocean? Geology 38:175-178. https://doi.org/10.1130/G30528.1

Tollmann A (1960) Die Hallstätterzone des östlichen Salzkammergutes und ihr Rahmen. Jahrb Geol Budesanst 103:37-131.

Tollmann A (1964) Zur Frage der Fazies decken in den Nördlichen Kalkalpen und zur Einwurzelung der Hallstätter Zone (Ostalpen). Geol Rund 53:153-170.

Tollmann A (1976a) Analyse des clasischen nordalpinen Mesozoikums: Stratigraphie, Fauna und Fazies der Nördlichen Kalkalpen. Franz Deuticke, Vienna.

Tollmann A (1976b) Der Bau der Nördlichen Kalkalpen: Orogene Stellung und regionale Tektonik. Franz Deuticke, Vienna.

Tollmann A (1981) Oberjurassische Gleittektonik als Hauptformungsprozeß der Hallstätter Region und neue Daten zur Gesamttektonik der Nördlichen Kalkalpen in den Ostalpen. Mitt Österr Geol Ges 74/75:167-195.

Vendeville BC, Jackson MPA (1992) The fall of diapirs during thin-skinned extension. Mar Petr Geol 9:354-371.

Wagreich M, Decker K (2001) Sedimentary tectonics and subsidence modelling of the type Upper Cretaceous Gosau basin (Northern Calcareous Alps, Austria). Int Jour Earth Sci 90:714-726. https://doi.org/10.1007/s005310000181

Zankl H (1967) Die Karbonatsedimente der Obertrias in den nördlichen Kalkalpen. Geol Rund 56:128-139.

Fig. 1

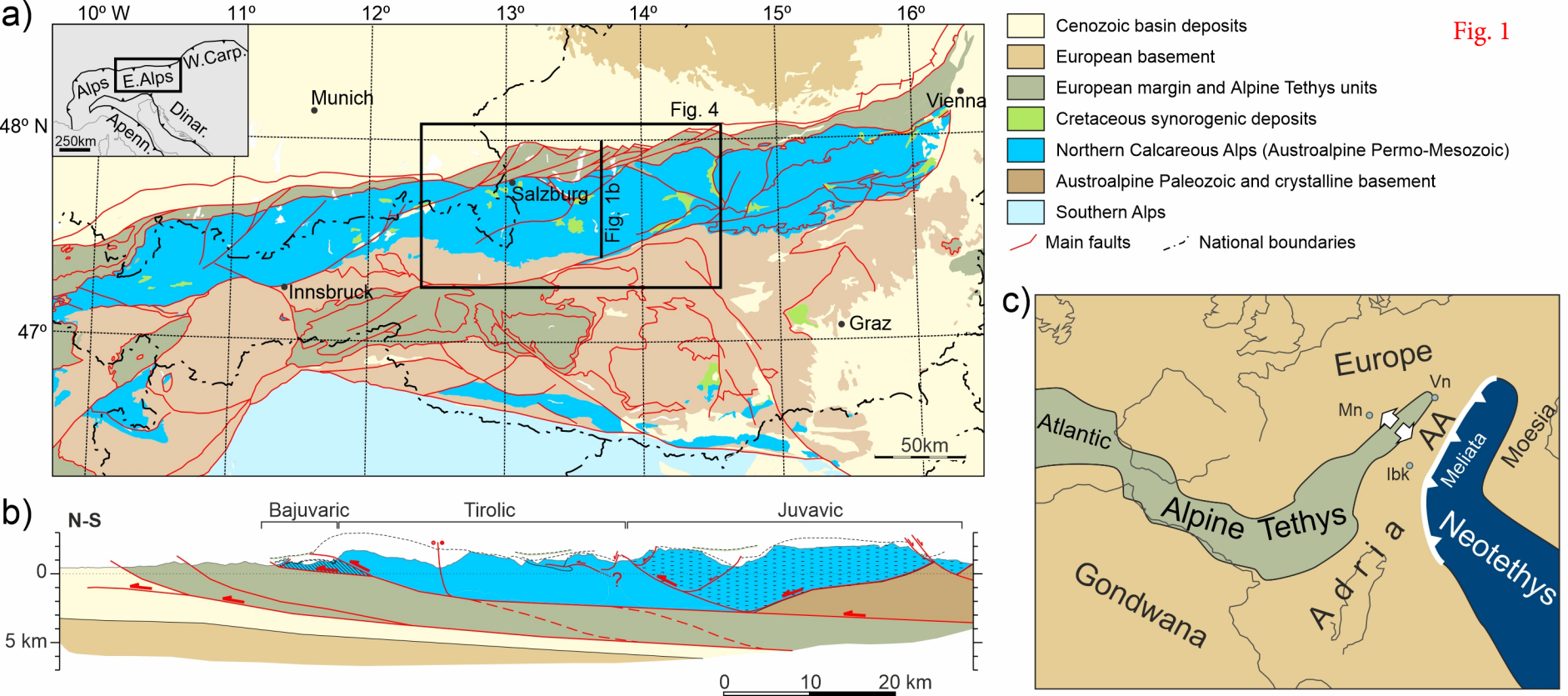
a)
10° W
11°
12°
13°
14°
15°
16°
48° N
47°
Alps
E.Alps
W.Carp.
Apenn.
Dinar.
250km
Munich
Fig. 4
Vienna
Salzburg
Fig. 1b
Innsbruck
Graz
50km
Cenozoic basin deposits
European basement
European margin and Alpine Tethys units
Cretaceous synorogenic deposits
Northern Calcareous Alps (Austroalpine Permo-Mesozoic)
Austroalpine Paleozoic and crystalline basement
Southern Alps
Main faults
National boundaries
b)
N-S
Bajuvaric
Tirolic
Juvavic
0
5 km
0
10
20 km
c)
Europe
Vn
Mn
Ibk
AA
Meliata
Moesia
Atlantic
Alpine Tethys
Adria
Neotethys
Gondwana

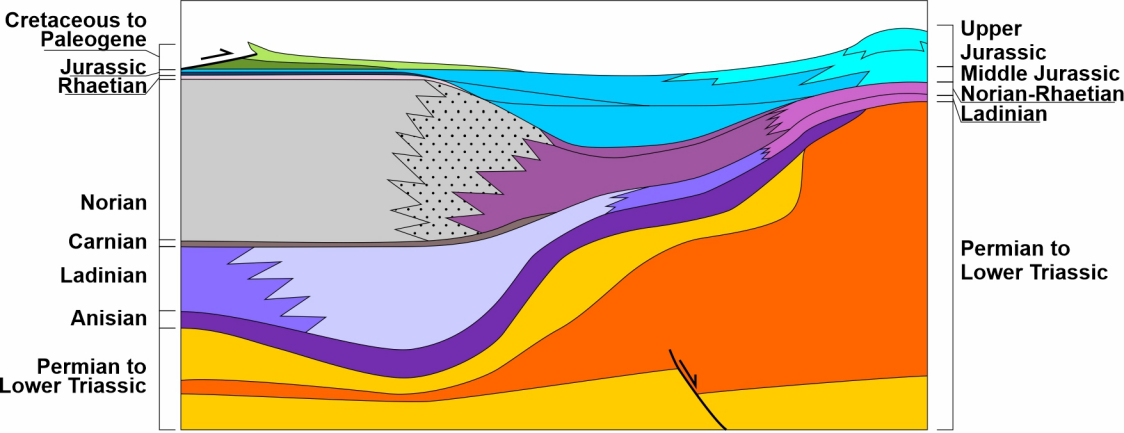
Cretaceous to Paleogene
Jurassic
Rhaetian
Norian
Carnian
Ladinian
Anisian
Permian to Lower Triassic
Upper Jurassic
Middle Jurassic
Norian-Rhaetian
Ladinian
Permian to Lower Triassic

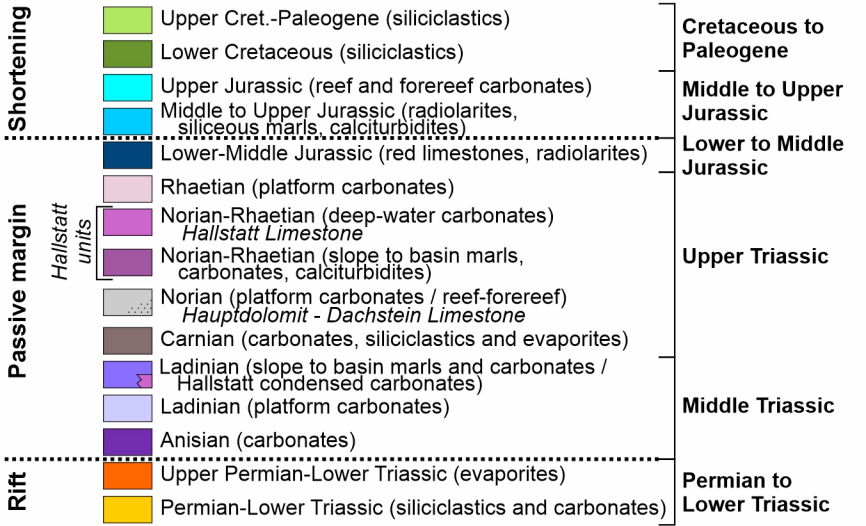
Shortening
Passive margin
Hallstatt units
Rift
Upper Cret.-Paleogene (siliciclastics)
Lower Cretaceous (siliciclastics)
Upper Jurassic (reef and forereef carbonates)
Middle to Upper Jurassic (radiolarites, siliceous marls, calciturbidites)
Lower-Middle Jurassic (red limestones, radiolarites)
Rhaetian (platform carbonates)
Norian-Rhaetian (deep-water carbonates)
Hallstatt Limestone
Norian-Rhaetian (slope to basin marls, carbonates, calciturbidites)
Norian (platform carbonates / reef-forereef)
Hauptdolomit - Dachstein Limestone
Carnian (carbonates, siliciclastics and evaporites)
Ladinian (slope to basin marls and carbonates / Hallstatt condensed carbonates)
Ladinian (platform carbonates)
Anisian (carbonates)
Upper Permian-Lower Triassic (evaporites)
Permian-Lower Triassic (siliciclastics and carbonates)
Cretaceous to Paleogene
Middle to Upper Jurassic
Lower to Middle Jurassic
Upper Triassic
Middle Triassic
Permian to Lower Triassic

Fig. 2

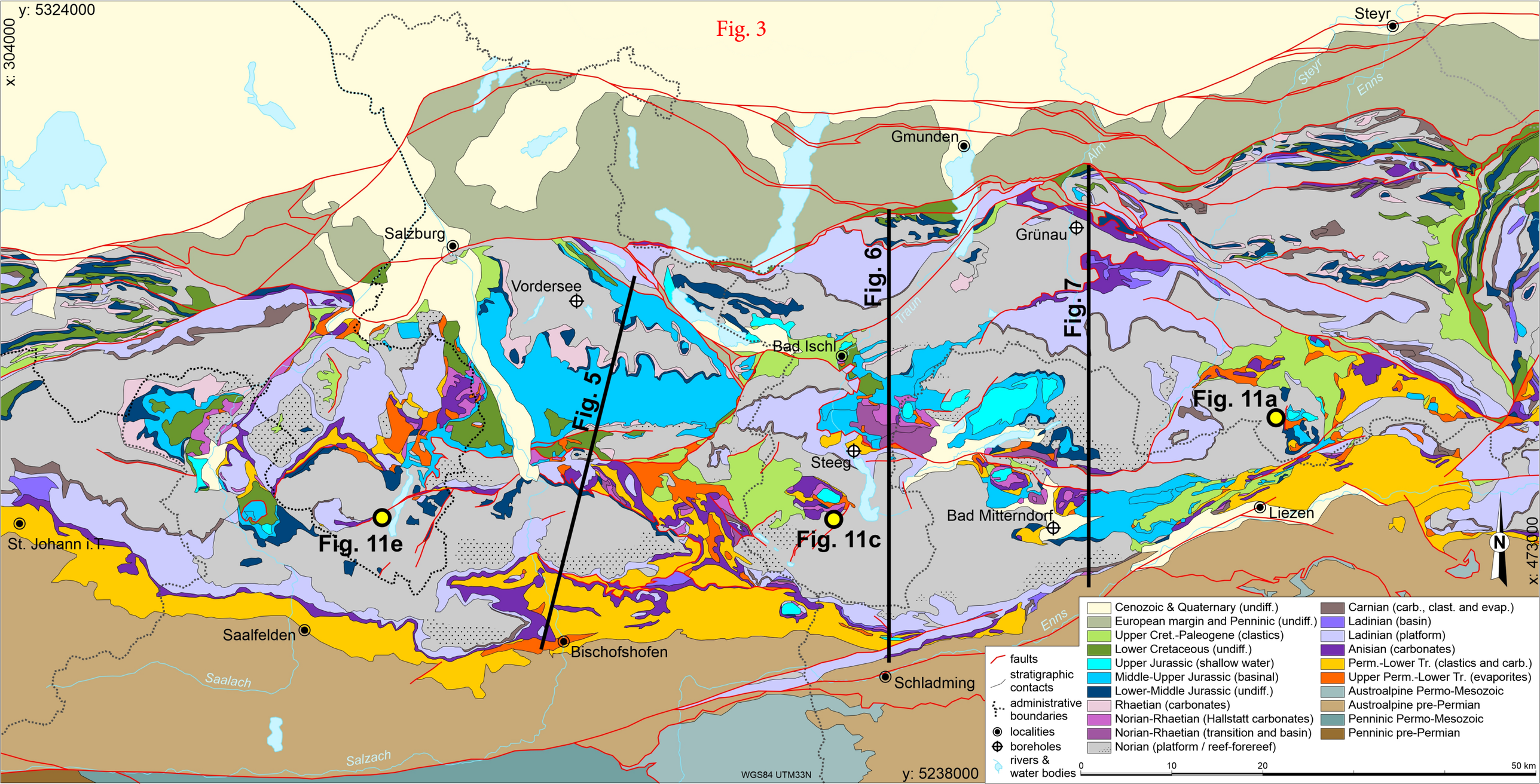
Fig. 3
y: 5324000
x: 304000
y: 5238000
x: 473000
Steyr
Gmunden
Salzburg
Vordersee
Grünau
Bad Ischl
Steeg
Bad Mitterndorf
Liezen
St. Johann i.T.
Saalfelden
Bischofshofen
Schladming
Fig. 5
Fig. 6
Fig. 7
Fig. 11a
Fig. 11c
Fig. 11e
Steyr
Enns
Alm
Traun
Saalach
Salzach
WGS84 UTM33N
N
faults
stratigraphic contacts
administrative boundaries
localities
boreholes
rivers & water bodies
Cenozoic & Quaternary (undiff.)
European margin and Penninic (undiff.)
Upper Cret.-Paleogene (clastics)
Lower Cretaceous (undiff.)
Upper Jurassic (shallow water)
Middle-Upper Jurassic (basinal)
Lower-Middle Jurassic (undiff.)
Rhaetian (carbonates)
Norian-Rhaetian (Hallstatt carbonates)
Norian-Rhaetian (transition and basin)
Norian (platform / reef-forereef)
Carnian (carb., clast. and evap.)
Ladinian (basin)
Ladinian (platform)
Anisian (carbonates)
Perm.-Lower Tr. (clastics and carb.)
Upper Perm.-Lower Tr. (evaporites)
Austroalpine Permo-Mesozoic
Austroalpine pre-Permian
Penninic Permo-Mesozoic
Penninic pre-Permian
0
10
20
50 km

Fig. 4

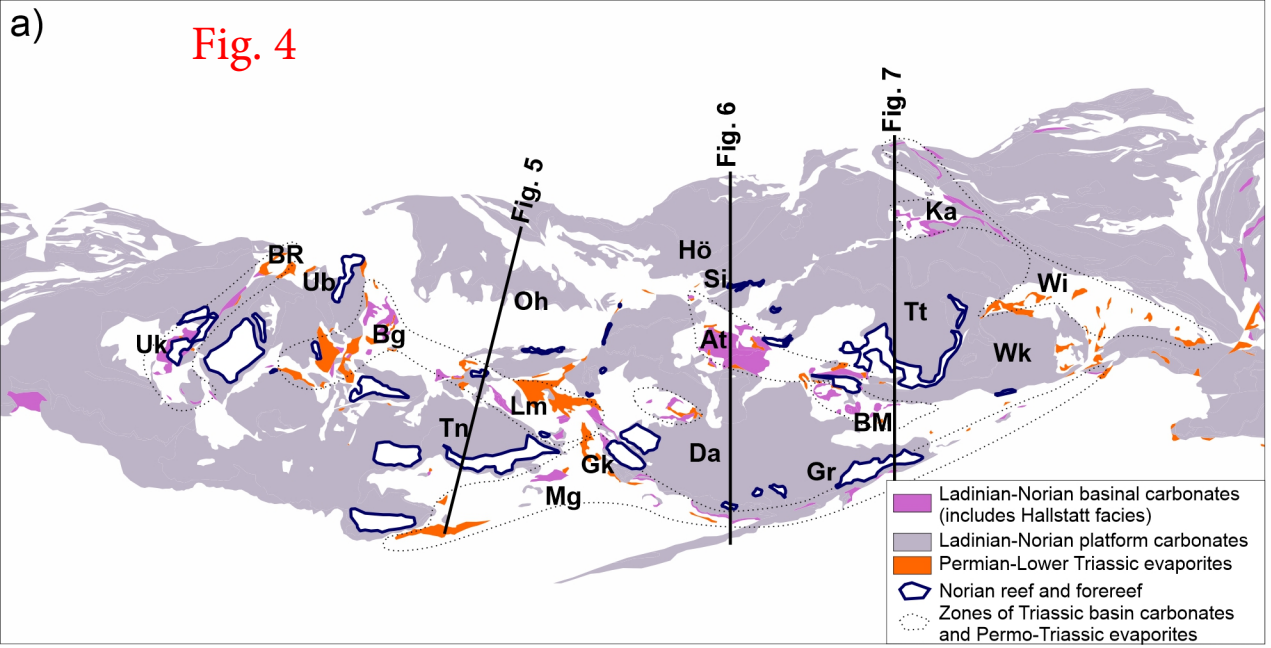
a)
Fig. 5
Fig. 6
Fig. 7
BR
Ub
Uk
Bg
Oh
Hö
Si
At
Ka
Wi
Tt
Wk
Lm
Tn
Gk
Da
BM
Gr
Mg
Ladinian-Norian basinal carbonates (includes Hallstatt facies)
Ladinian-Norian platform carbonates
Permian-Lower Triassic evaporites
Norian reef and forereef
Zones of Triassic basin carbonates and Permo-Triassic evaporites

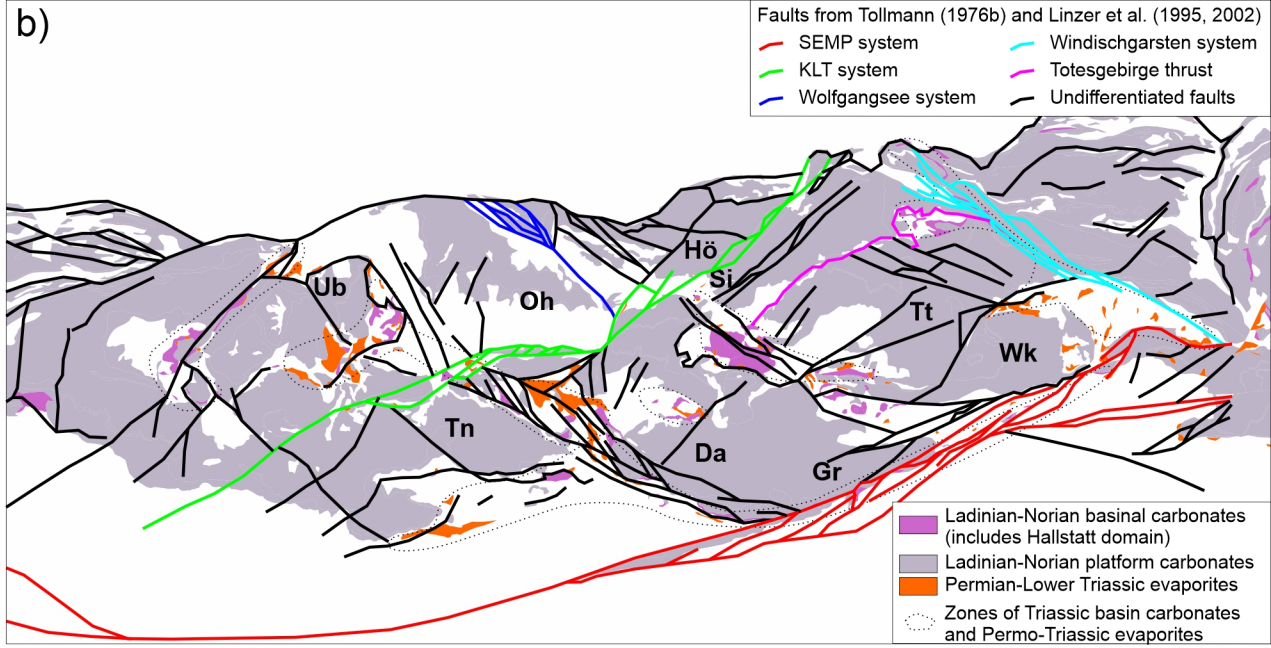
b)
Faults from Tollmann (1976b) and Linzer et al. (1995, 2002)
SEMP system
KLT system
Wolfgangsee system
Windischgarsten system
Totesgebirge thrust
Undifferentiated faults
Ub
Oh
Hö
Si
Tt
Wk
Tn
Da
Gr
Ladinian-Norian basinal carbonates (includes Hallstatt domain)
Ladinian-Norian platform carbonates
Permian-Lower Triassic evaporites
Zones of Triassic basin carbonates and Permo-Triassic evaporites

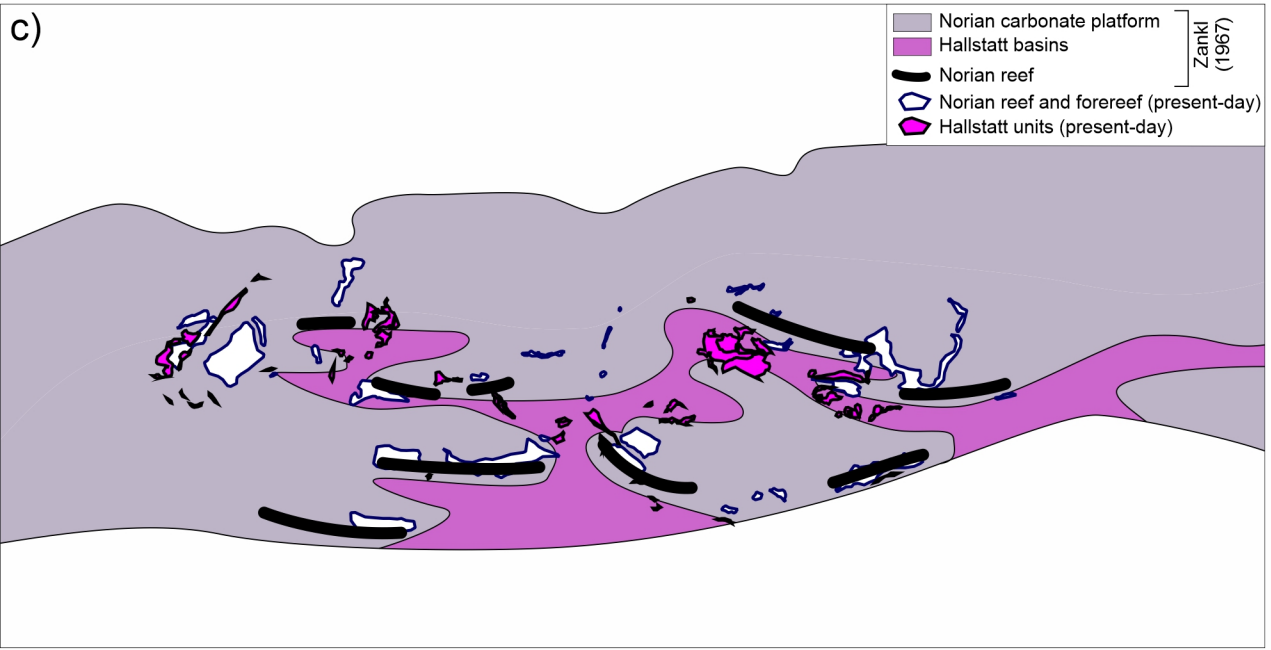
c)
Norian carbonate platform
Hallstatt basins
Norian reef
Zankl (1967)
Norian reef and forereef (present-day)
Hallstatt units (present-day)

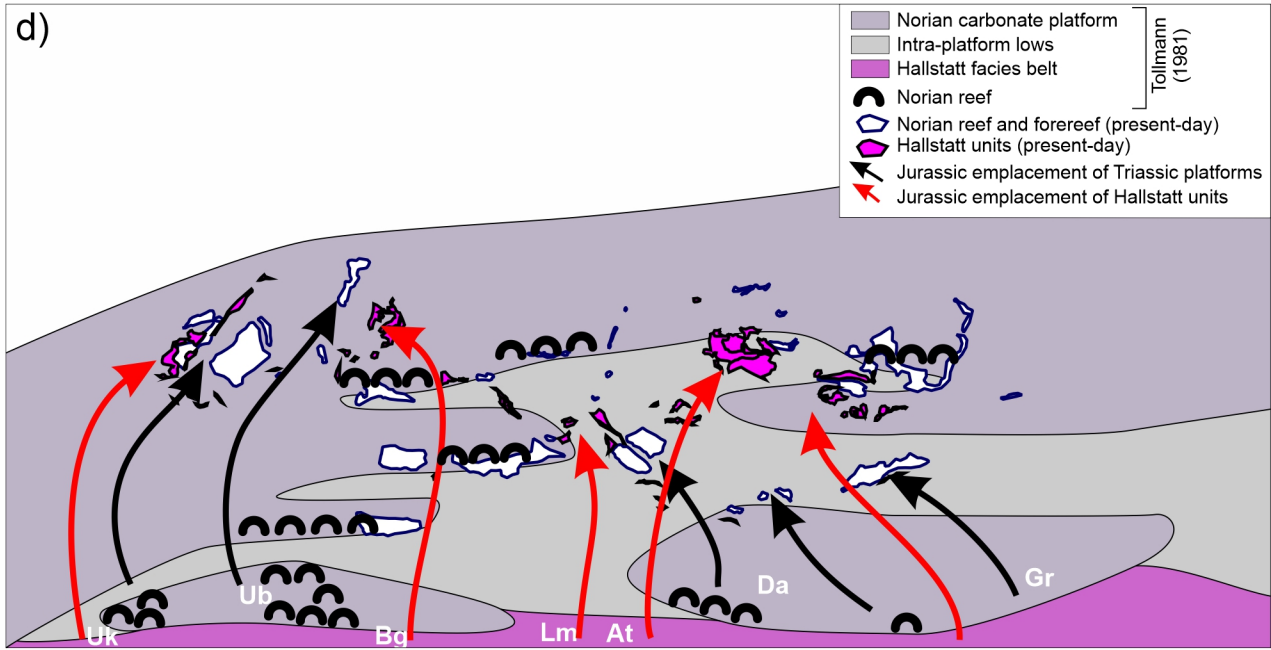
d)
Norian carbonate platform
Intra-platform lows
Hallstatt facies belt
Norian reef
Tollmann (1981)
Norian reef and forereef (present-day)
Hallstatt units (present-day)
Jurassic emplacement of Triassic platforms
Jurassic emplacement of Hallstatt units
Uk
Ub
Bg
Lm
At
Da
Gr

Fig. 5

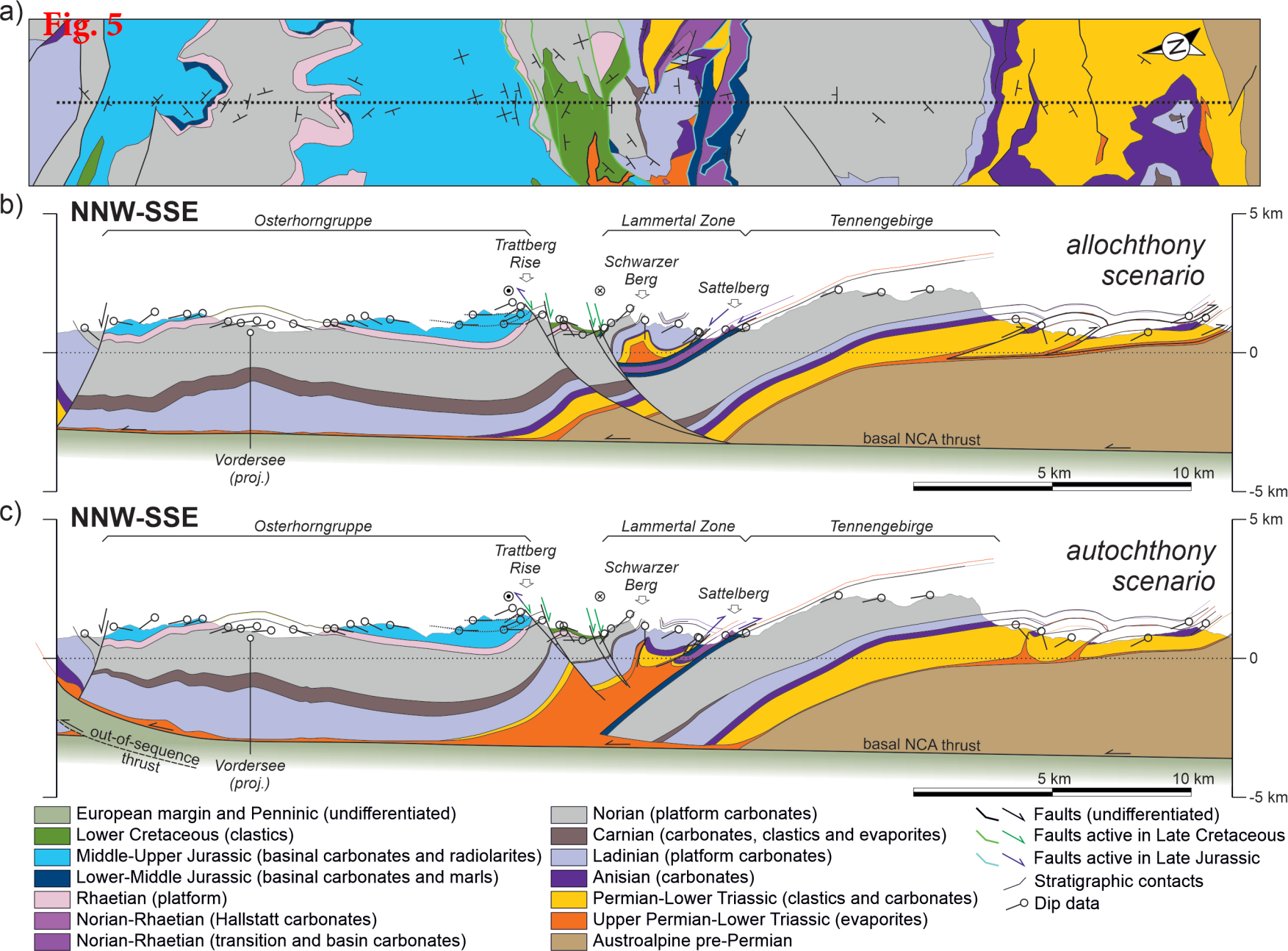
a)
N
b)
NNW-SSE
Osterhorngruppe
Lammertal Zone
Tennengebirge
Trattberg Rise
Schwarzer Berg
Sattelberg
allochthony scenario
5 km
0
-5 km
basal NCA thrust
Vordersee (proj.)
5 km
10 km
c)
NNW-SSE
Osterhorngruppe
Lammertal Zone
Tennengebirge
Trattberg Rise
Schwarzer Berg
Sattelberg
autochthony scenario
5 km
0
-5 km
basal NCA thrust
out-of-sequence thrust
Vordersee (proj.)
5 km
10 km
European margin and Penninic (undifferentiated)
Lower Cretaceous (clastics)
Middle-Upper Jurassic (basinal carbonates and radiolarites)
Lower-Middle Jurassic (basinal carbonates and marls)
Rhaetian (platform)
Norian-Rhaetian (Hallstatt carbonates)
Norian-Rhaetian (transition and basin carbonates)
Norian (platform carbonates)
Carnian (carbonates, clastics and evaporites)
Ladinian (platform carbonates)
Anisian (carbonates)
Permian-Lower Triassic (clastics and carbonates)
Upper Permian-Lower Triassic (evaporites)
Austroalpine pre-Permian
Faults (undifferentiated)
Faults active in Late Cretaceous
Faults active in Late Jurassic
Stratigraphic contacts
Dip data

Fig. 6

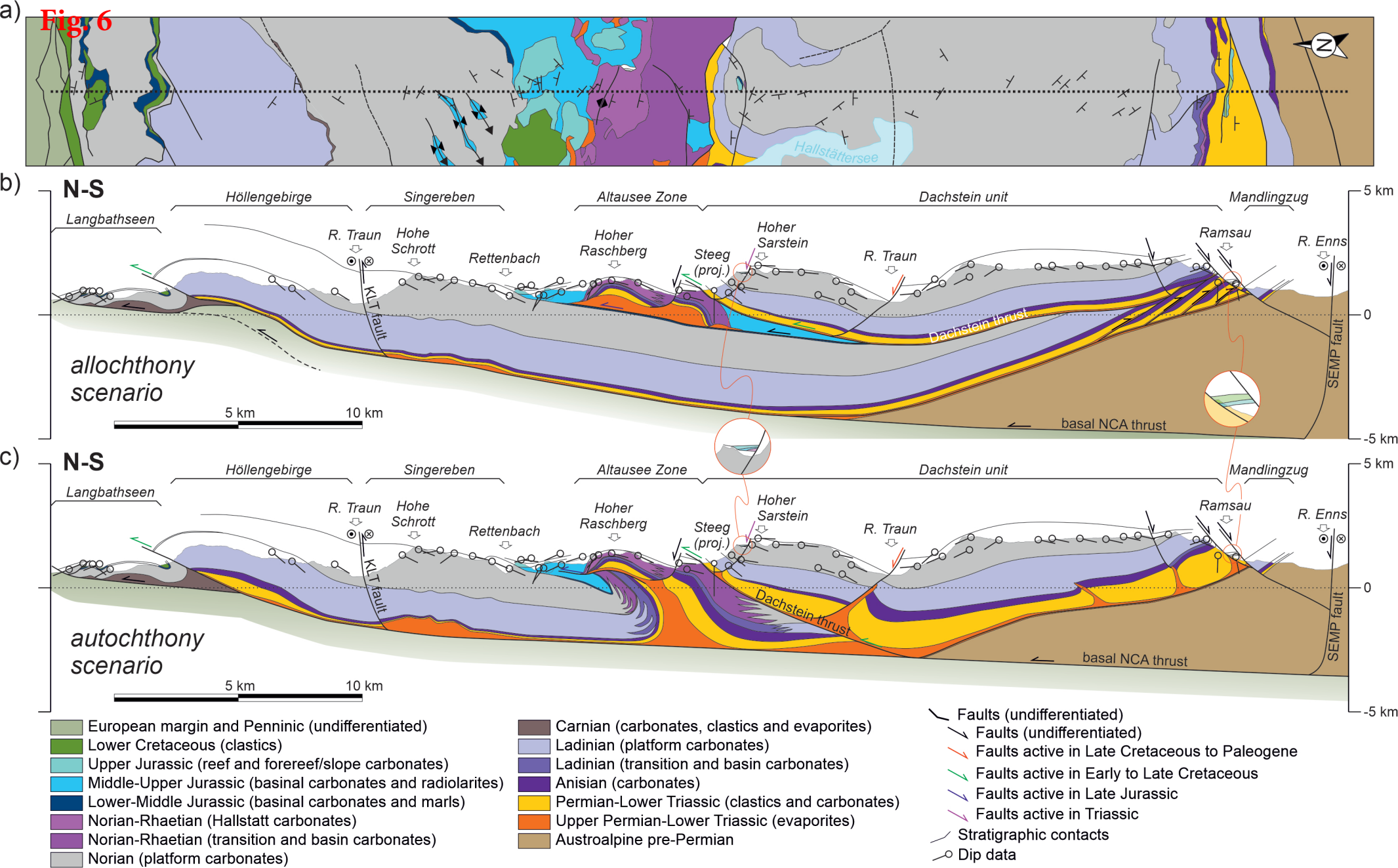
a)
Hallstättersee
N
b)
N-S
Höllengebirge
Singereben
Altausee Zone
Dachstein unit
Mandlingzug
Langbathseen
R. Traun
Hohe Schrott
Rettenbach
Hoher Raschberg
Steeg (proj.)
Hoher Sarstein
R. Traun
Ramsau
R. Enns
KLT fault
Dachstein thrust
SEMP fault
basal NCA thrust
allochthony scenario
5 km
10 km
5 km
0
-5 km
c)
N-S
Höllengebirge
Singereben
Altausee Zone
Dachstein unit
Mandlingzug
Langbathseen
R. Traun
Hohe Schrott
Rettenbach
Hoher Raschberg
Steeg (proj.)
Hoher Sarstein
R. Traun
Ramsau
R. Enns
KLT fault
Dachstein thrust
SEMP fault
basal NCA thrust
autochthony scenario
5 km
10 km
5 km
0
-5 km
European margin and Penninic (undifferentiated)
Lower Cretaceous (clastics)
Upper Jurassic (reef and forereef/slope carbonates)
Middle-Upper Jurassic (basinal carbonates and radiolarites)
Lower-Middle Jurassic (basinal carbonates and marls)
Norian-Rhaetian (Hallstatt carbonates)
Norian-Rhaetian (transition and basin carbonates)
Norian (platform carbonates)
Carnian (carbonates, clastics and evaporites)
Ladinian (platform carbonates)
Ladinian (transition and basin carbonates)
Anisian (carbonates)
Permian-Lower Triassic (clastics and carbonates)
Upper Permian-Lower Triassic (evaporites)
Austroalpine pre-Permian
Faults (undifferentiated)
Faults (undifferentiated)
Faults active in Late Cretaceous to Paleogene
Faults active in Early to Late Cretaceous
Faults active in Late Jurassic
Faults active in Triassic
Stratigraphic contacts
Dip data

Fig. 7

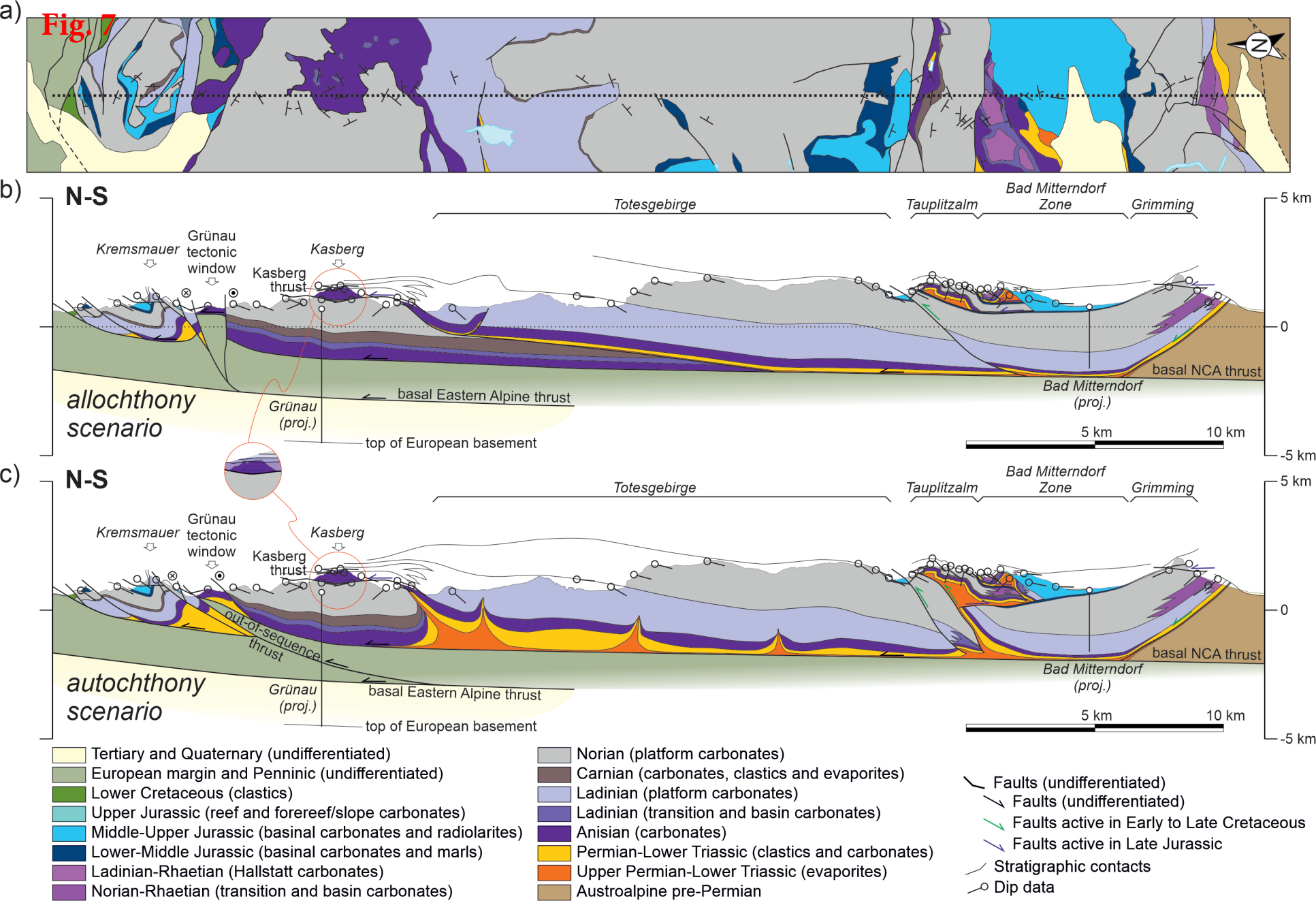
a)
N
b)
N-S
Totesgebirge
Tauplitzalm
Bad Mitterndorf Zone
Grimming
Kremsmauer
Grünau tectonic window
Kasberg
Kasberg thrust
basal NCA thrust
Bad Mitterndorf (proj.)
allochthony scenario
Grünau (proj.)
basal Eastern Alpine thrust
top of European basement
5 km
10 km
5 km
0
-5 km
c)
N-S
Totesgebirge
Tauplitzalm
Bad Mitterndorf Zone
Grimming
Kremsmauer
Grünau tectonic window
Kasberg
Kasberg thrust
out-of-sequence thrust
basal NCA thrust
Bad Mitterndorf (proj.)
autochthony scenario
Grünau (proj.)
basal Eastern Alpine thrust
top of European basement
5 km
10 km
5 km
0
-5 km
Tertiary and Quaternary (undifferentiated)
European margin and Penninic (undifferentiated)
Lower Cretaceous (clastics)
Upper Jurassic (reef and forereef/slope carbonates)
Middle-Upper Jurassic (basinal carbonates and radiolarites)
Lower-Middle Jurassic (basinal carbonates and marls)
Ladinian-Rhaetian (Hallstatt carbonates)
Norian-Rhaetian (transition and basin carbonates)
Norian (platform carbonates)
Carnian (carbonates, clastics and evaporites)
Ladinian (platform carbonates)
Ladinian (transition and basin carbonates)
Anisian (carbonates)
Permian-Lower Triassic (clastics and carbonates)
Upper Permian-Lower Triassic (evaporites)
Austroalpine pre-Permian
Faults (undifferentiated)
Faults (undifferentiated)
Faults active in Early to Late Cretaceous
Faults active in Late Jurassic
Stratigraphic contacts
Dip data

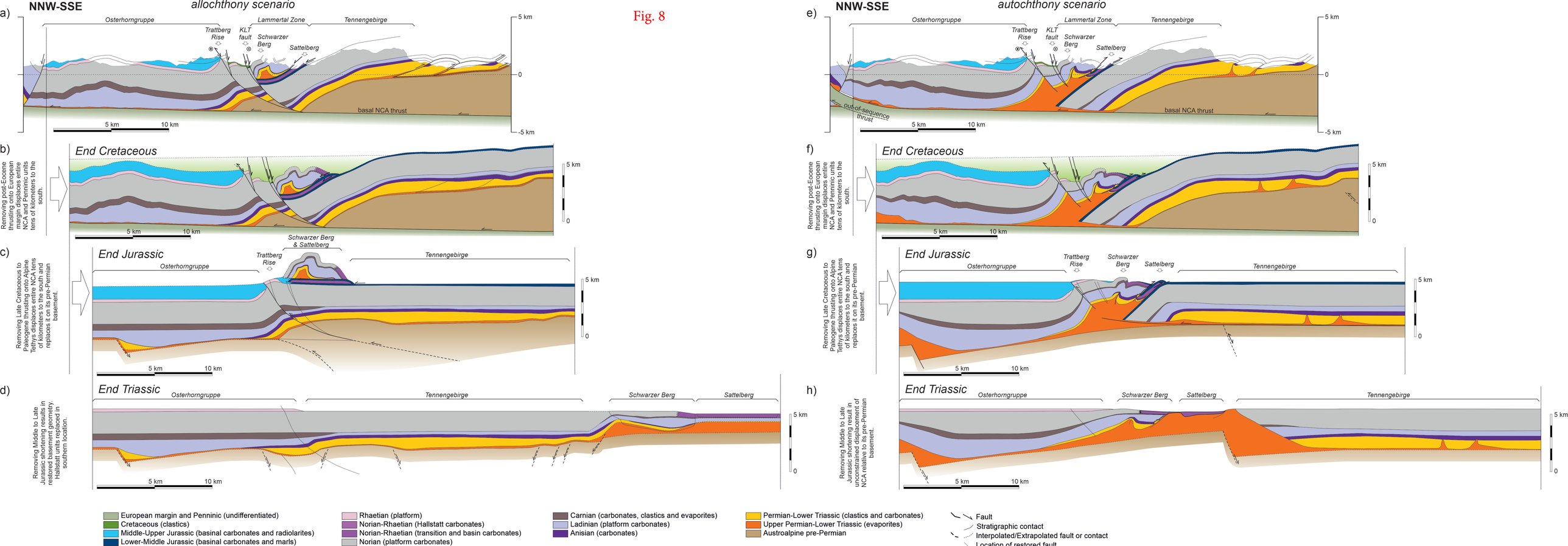
Fig. 8
a)
NNW-SSE
allochthony scenario
Osterhorngruppe
Lammertal Zone
Tennengebirge
Trattberg Rise
KLT fault
Schwarzer Berg
Sattelberg
5 km
0
-5 km
basal NCA thrust
5 km
10 km
b)
Removing post-Eocene thrusting onto European margin displaces entire Northern Calcareous Alps tens of kilometers to the south.
End Cretaceous
5 km
0
5 km
10 km
c)
Removing Late Cretaceous to Paleogene thrusting onto Alpine Tethys displaces entire NCA tens of kilometers to the south and replaces it on its pre-Permian basement.
End Jurassic
Schwarzer Berg & Sattelberg
Trattberg Rise
Osterhorngruppe
Tennengebirge
5 km
0
5 km
10 km
d)
Removing Middle to Late Jurassic shortening results in restored Jurassic basement (mostly Hallstatt units replaced in southern location.
End Triassic
Osterhorngruppe
Tennengebirge
Schwarzer Berg
Sattelberg
5 km
0
5 km
10 km
e)
NNW-SSE
autochthony scenario
Osterhorngruppe
Lammertal Zone
Tennengebirge
Trattberg Rise
KLT fault
Schwarzer Berg
Sattelberg
5 km
0
-5 km
out-of-sequence thrust
basal NCA thrust
5 km
10 km
f)
Removing post-Eocene thrusting onto European margin displaces entire NCA and Penninic units tens of kilometers to the south.
End Cretaceous
5 km
0
5 km
10 km
g)
Removing Late Cretaceous to Paleogene thrusting onto Alpine Tethys displaces entire NCA tens of kilometers to the south and replaces it on its pre-Permian basement.
End Jurassic
Osterhorngruppe
Trattberg Rise
Schwarzer Berg
Sattelberg
Tennengebirge
5 km
0
5 km
10 km
h)
Removing Middle to Late Jurassic shortening result in unconstrained displacement of NCA relative to its pre-Permian basement.
End Triassic
Osterhorngruppe
Schwarzer Berg
Sattelberg
Tennengebirge
5 km
0
5 km
10 km
European margin and Penninic (undifferentiated)
Cretaceous (clastics)
Middle-Upper Jurassic (basinal carbonates and radiolarites)
Lower-Middle Jurassic (basinal carbonates and marls)
Rhaetian (platform)
Norian-Rhaetian (Hallstatt carbonates)
Norian-Rhaetian (transition and basin carbonates)
Norian (platform carbonates)
Carnian (carbonates, clastics and evaporites)
Ladinian (platform carbonates)
Anisian (carbonates)
Permian-Lower Triassic (clastics and carbonates)
Upper Permian-Lower Triassic (evaporites)
Austroalpine pre-Permian
Fault
Stratigraphic contact
Interpolated/Extrapolated fault or contact
Location of restored fault

Fig. 9

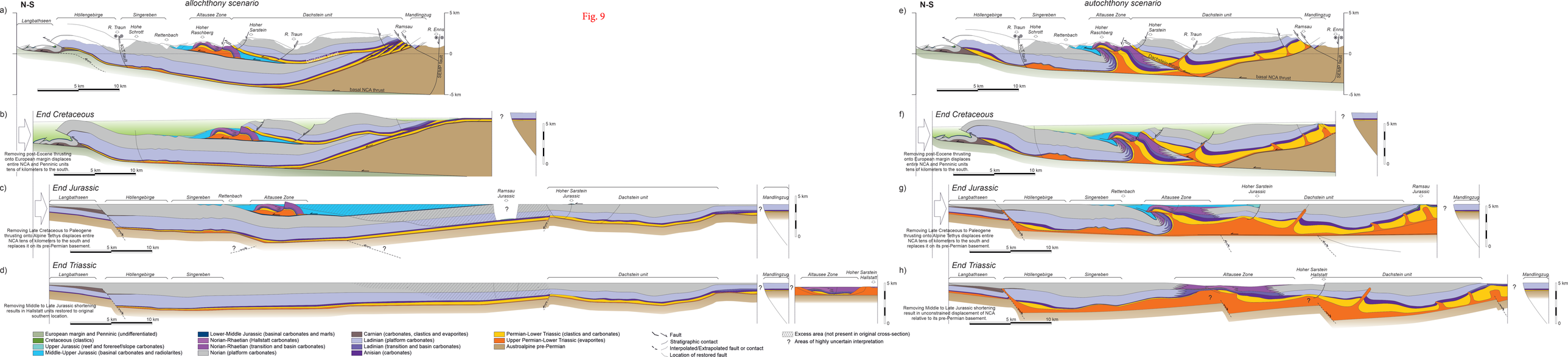
a)
N-S
allochthony scenario
Langbathseen
Höllengebirge
Singereben
Altausee Zone
Dachstein unit
Mandlingzug
R. Traun
Hohe Schrott
Rettenbach
Hoher Raschberg
Hoher Sarstein
R. Traun
Ramsau
R. Enns
5 km
0
-5 km
5 km
10 km
basal NCA thrust
SEMP fault
b)
End Cretaceous
Removing post-Eocene thrusting onto European margin displaces entire NCA and Penninic units tens of kilometers to the south.
c)
End Jurassic
Ramsau Jurassic
Hoher Sarstein Jurassic
Removing Late Cretaceous to Paleogene thrusting onto Alpine Tethys displaces entire NCA tens of kilometers to the south and replaces it on its pre-Permian basement.
d)
End Triassic
Hallstatt
Removing Middle to Late Jurassic shortening results in Hallstatt units restored to original southern location.
e)
N-S
autochthony scenario
Dachstein thrust
f)
End Cretaceous
Removing post-Eocene thrusting onto European margin displaces entire NCA and Penninic units tens of kilometers to the south.
g)
End Jurassic
Removing Late Cretaceous to Paleogene thrusting onto Alpine Tethys displaces entire NCA tens of kilometers to the south and replaces it on its pre-Permian basement.
h)
End Triassic
Hallstatt
Removing Middle to Late Jurassic shortening result in unconstrained displacement of NCA relative to its pre-Permian basement.
European margin and Penninic (undifferentiated)
Cretaceous (clastics)
Upper Jurassic (reef and forereef/slope carbonates)
Middle-Upper Jurassic (basinal carbonates and radiolarites)
Lower-Middle Jurassic (basinal carbonates and marls)
Norian-Rhaetian (Hallstatt carbonates)
Norian-Rhaetian (transition and basin carbonates)
Norian (platform carbonates)
Carnian (carbonates, clastics and evaporites)
Ladinian (platform carbonates)
Ladinian (transition and basin carbonates)
Anisian (carbonates)
Permian-Lower Triassic (clastics and carbonates)
Upper Permian-Lower Triassic (evaporites)
Austroalpine pre-Permian
Fault
Stratigraphic contact
Interpolated/Extrapolated fault or contact
Location of restored fault
Excess area (not present in original cross-section)
? Areas of highly uncertain interpretation

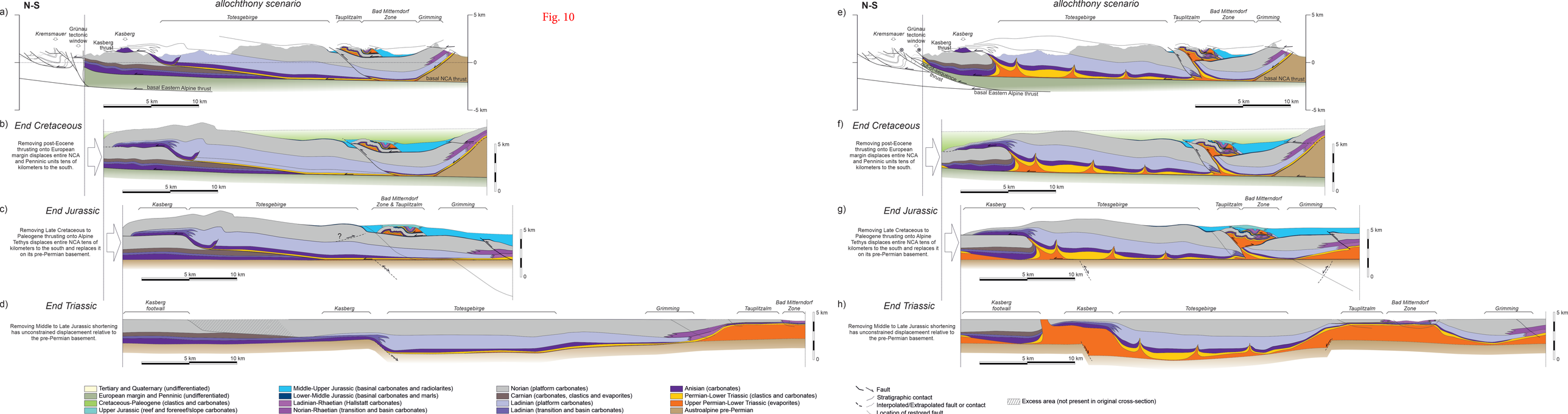
a)
N-S
allochthony scenario
Totesgebirge
Tauplitzalm
Bad Mitterndorf Zone
Grimming
Kremsmauer
Grünau tectonic window
Kasberg
Kasberg thrust
5 km
0
-5 km
basal NCA thrust
basal Eastern Alpine thrust
5 km
10 km
b)
End Cretaceous
Removing post-Eocene thrusting onto European margin displaces entire NCA and Penninic units tens of kilometers to the south.
c)
End Jurassic
Removing Late Cretaceous to Paleogene thrusting onto Alpine Tethys displaces entire NCA tens of kilometers to the south and replaces it on its pre-Permian basement.
Bad Mitterndorf Zone & Tauplitzalm
?
d)
End Triassic
Removing Middle to Late Jurassic shortening has unconstrained displacemeent relative to the pre-Permian basement.
Kasberg footwall
e)
Allochthonous thrust
f)
g)
h)
Tertiary and Quaternary (undifferentiated)
European margin and Penninic (undifferentiated)
Cretaceous-Paleogene (clastics and carbonates)
Upper Jurassic (reef and forereef/slope carbonates)
Middle-Upper Jurassic (basinal carbonates and radiolarites)
Lower-Middle Jurassic (basinal carbonates and marls)
Ladinian-Rhaetian (Hallstatt carbonates)
Norian-Rhaetian (transition and basin carbonates)
Norian (platform carbonates)
Carnian (carbonates, clastics and evaporites)
Ladinian (platform carbonates)
Ladinian (transition and basin carbonates)
Anisian (carbonates)
Permian-Lower Triassic (clastics and carbonates)
Upper Permian-Lower Triassic (evaporites)
Austroalpine pre-Permian
Fault
Stratigraphic contact
Interpolated/Extrapolated fault or contact
Location of restored fault
Excess area (not present in original cross-section)

Fig. 10

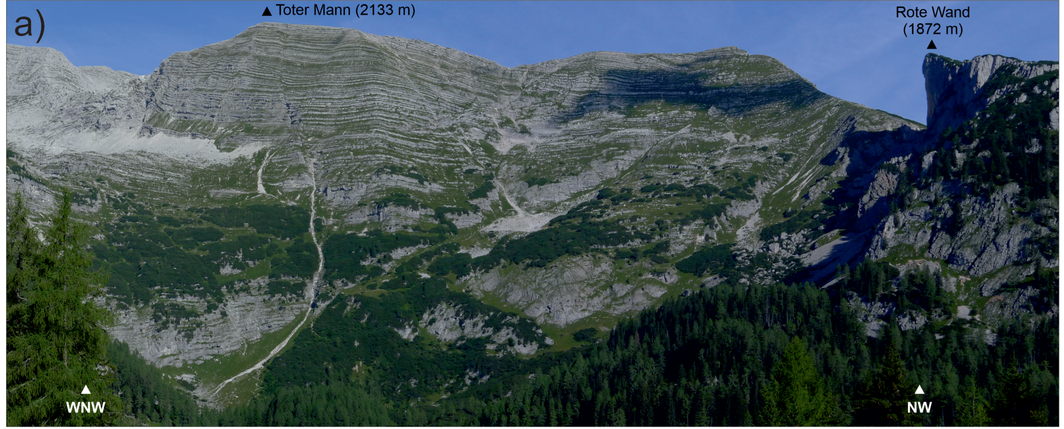
a)
▲Toter Mann (2133 m)
Rote Wand
(1872 m)
▲
WNW
▲
NW

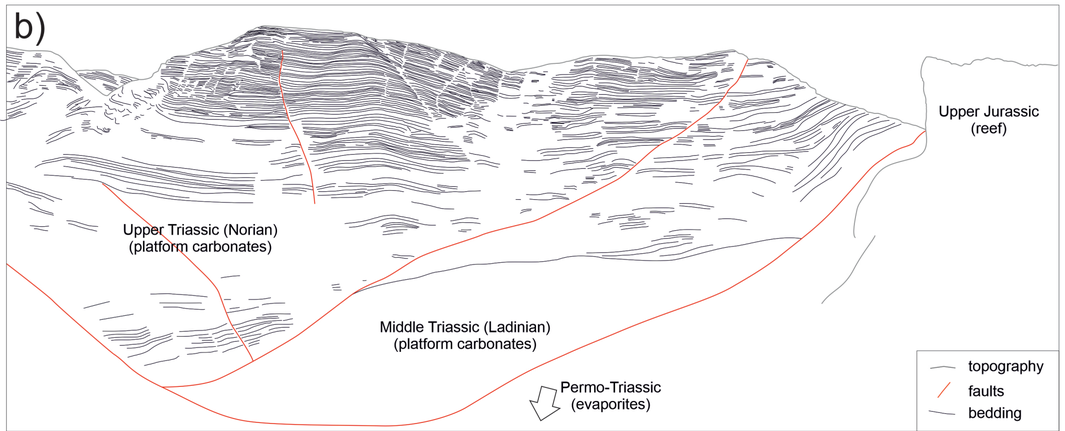
b)
Upper Jurassic
(reef)
Upper Triassic (Norian)
(platform carbonates)
Middle Triassic (Ladinian)
(platform carbonates)
Permo-Triassic
(evaporites)
topography
faults
bedding

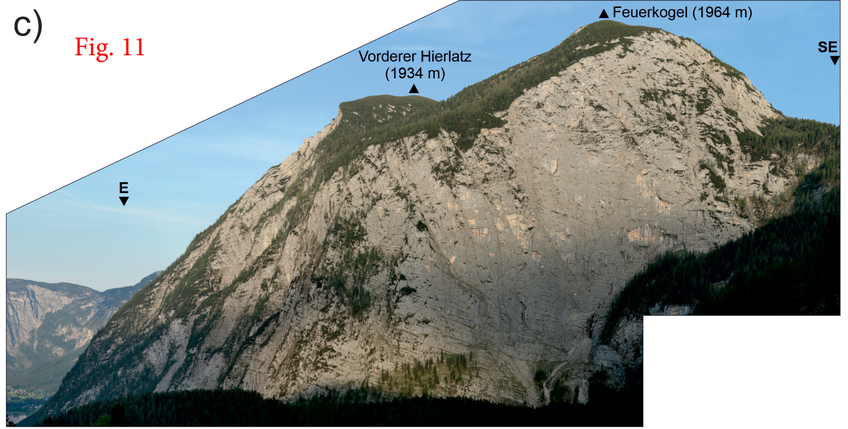
c)
Fig. 11
▲Feuerkogel (1964 m)
Vorderer Hierlatz
(1934 m)
SE
E


d)
Hallstatt diapir
(~ 1km)
topography
faults
bedding
extent of N-S
striking wall


e)
Hachelkopf
(2066 m)
S
SE
Eisgraben

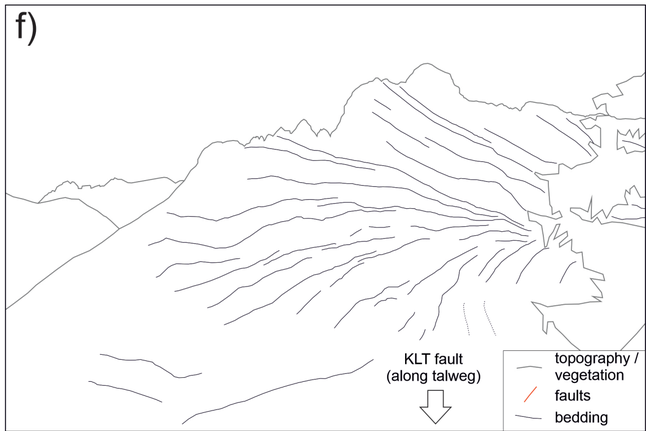
f)
KLT fault
(along talweg)
topography /
vegetation
faults
bedding

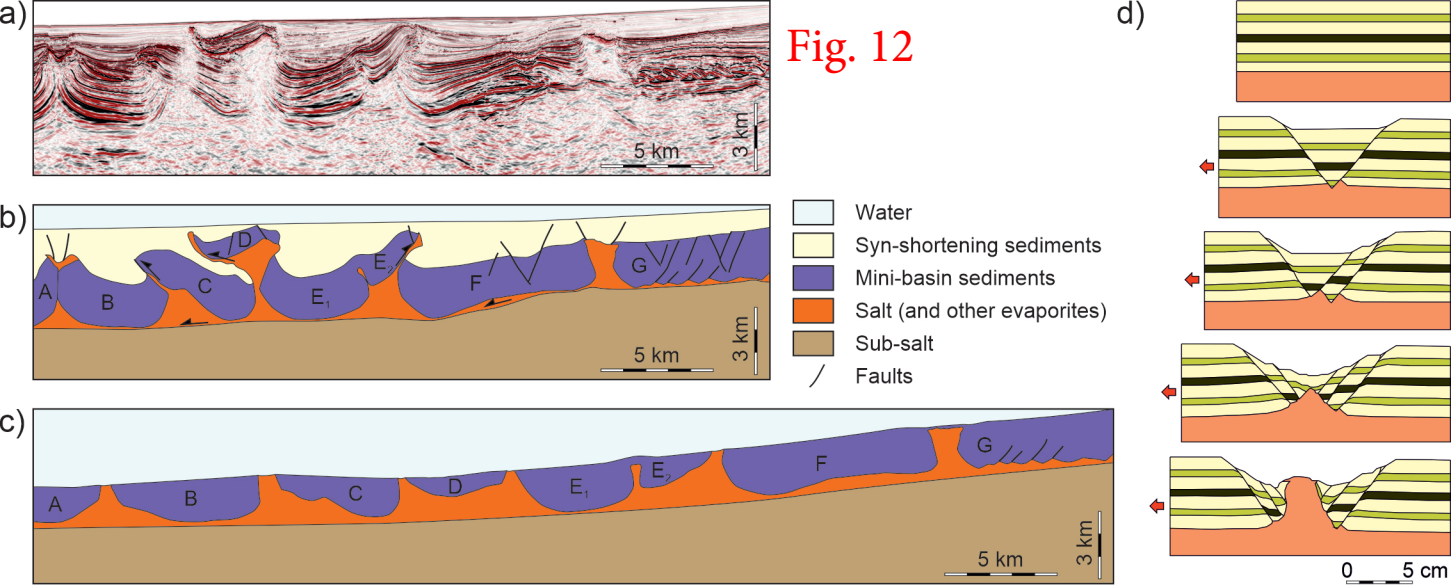
a)
5 km
3 km
b)
A
B
C
D
E1
E2
F
G
5 km
3 km
Water
Syn-shortening sediments
Mini-basin sediments
Salt (and other evaporites)
Sub-salt
Faults
c)
A
B
C
D
E1
E2
F
G
5 km
3 km
d)
0
5 cm

Fig. 12

Fig. 13

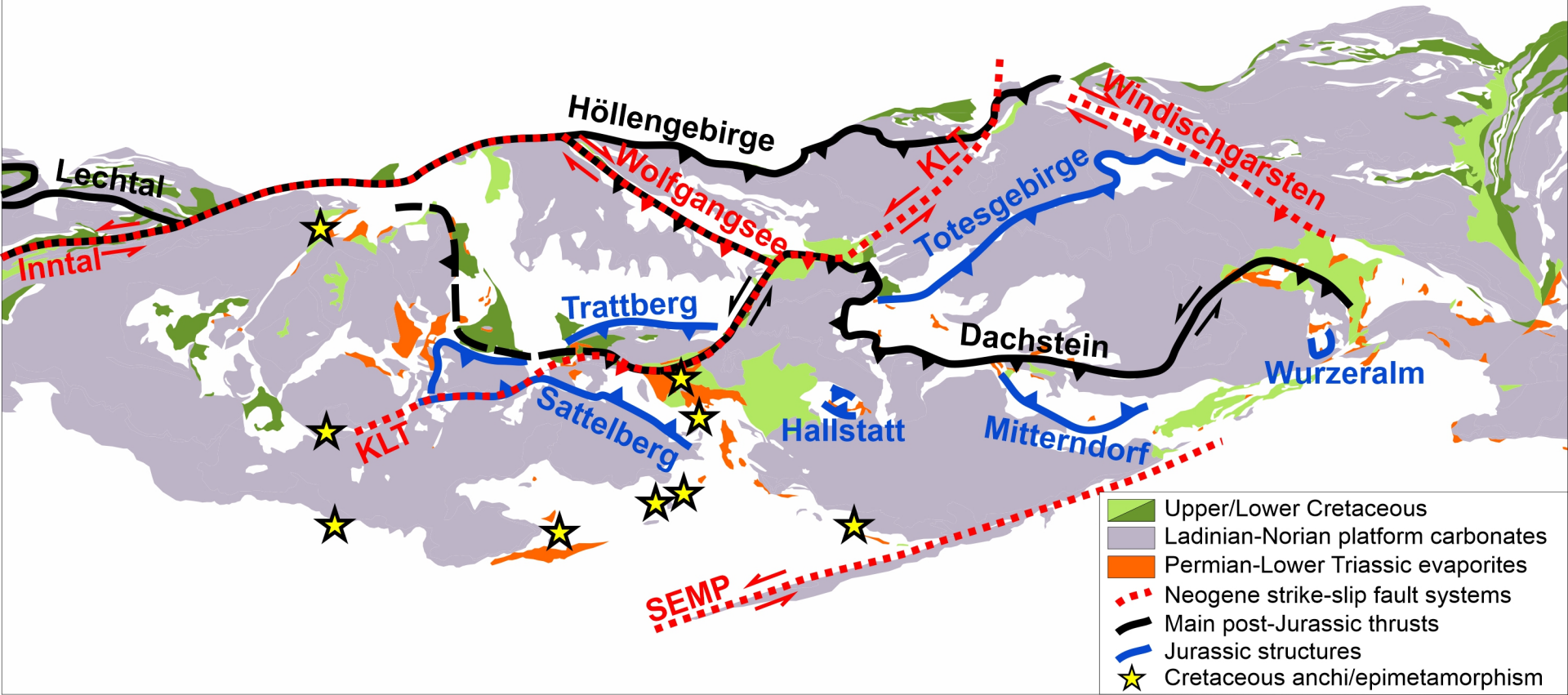
Höllengebirge
Lechtal
Inntal
Wolfgangsee
KLT
Windischgarsten
Totesgebirge
Trattberg
Dachstein
Wurzeralm
KLT
Sattelberg
Hallstatt
Mitterndorf
SEMP
Upper/Lower Cretaceous
Ladinian-Norian platform carbonates
Permian-Lower Triassic evaporites
Neogene strike-slip fault systems
Main post-Jurassic thrusts
Jurassic structures
Cretaceous anchi/epimetamorphism